UNIVERSIDADE FEDERAL DE SÃO CARLOS

CENTRO DE CIÊNCIAS EXATAS E DE TECNOLOGIA

DEPARTAMENTO DE ENGENHARIA DE MATERIAIS

FINITE ELEMENT SIMULATION FOR GLASS TEMPERING

ENZO HENRIQUE MIGUEL

SÃO CARLOS - SP
2024

FINITE ELEMENT SIMULATION FOR GLASS TEMPERING

Final report presented to the Materials Engineering Department of the Federal University of São Carlos as a requirement for the degree of Bachelor of Science in Materials Engineering.

Advisor: Prof. Vinicius Fiocco Sciuti

São Carlos - SP
2024

UNIVERSIDADE FEDERAL DE SÃO CARLOS
CENTRO DE CIÊNCIAS EXATAS E DE TECNOLOGIA
DEPARTAMENTO DE ENGENHARIA DE MATERIAIS
Telefones: 16 –3351-8244 e 3351-8246
Endereço eletrônico: demachef@ufscar.br
Rodovia Washington Luís, km 235 – Caixa Postal 676
CEP 13565-905 – São Carlos – SP - Brasil

ATA DE DEFESA DE TRABALHO DE CONCLUSÃO DE CURSO (TCC)

NOME: Enzo Henrique Miguel

RA: 759065

TÍTULO: Simulação em elementos finitos para a têmpera de vidros

ORIENTADOR(A): Prof. Dr. Vinícius Fiocco Sciuti

DATA/HORÁRIO: 02/02/2024, 14h30

BANCA – NOTAS:

	Monografia	Defesa
Prof. Dr. Vinícius Fiocco Sciuti	10,0	10,0
Prof. Dr. Rodrigo Bresciani Canto	10,0	10,0
Média	10,0	10,0

BANCA – ASSINATURAS:

gov.br Documento assinado digitalmente
VINICIUS FIOCCO SCIUTI
Data: 02/02/2024 17:55:33-0300
Verifique em https://validar.iti.gov.br

Prof. Dr. Vinícius Fiocco Sciuti _____

gov.br Documento assinado digitalmente
RODRIGO BRESCIANI CANTO
Data: 04/02/2024 08:59:17-0300
Verifique em https://validar.iti.gov.br

Prof. Dr. Rodrigo Bresciani Canto _____

ACKNOWLEDGMENT

First of all, I would like to thank my entire family for all their support: my father Paulo, who has always invested in my education, my mother Cristiane, who has always believed in me, my aunt and uncle Sylvana and Marcos, who have always worried about me, and my girlfriend Beatriz, who is my supporter and role model.

During my graduation, I had the privilege of learning from the best professionals. I would like to thank Prof. Vinícius Sciuti, my advisor in this work, Prof. Edgar Dutra Zanotto, my first advisor, and Débora Fabris, who guided me in my first steps as a researcher, and all my colleagues at LaMaV: Laurie, Laís, Helena, Geovana, Ricardo, Zé and all the others.

On this journey, I have been blessed with amazing friends who have supported me both in Brazil and in France. Many thanks to my close friends at UFSCar, Martinez, Vitor, Nathan, Eduardo, Maria Paula, Pedro, Marcelo, Carol and all the other members of the "Primas Mancilha" group, along with my childhood friends Senise, Gagui, Bruna and Flávia.

I would also like to thank DEMa, UFSCar, CAPES and my internship tutor Pierre Potigny for making it possible for me to fulfill my childhood dream of living in France and working at Airbus.

Finally, I would like to express my deep gratitude to the friends I made in France and the flatmates I had in Grenoble, Toulouse and Marseille: Akira, Yoann, Iris, Lisa and Julie. Many people find it difficult to adapt to another country, but thanks to them, as well as immersing myself in French culture, I feel that France has become part of me.

RESUMO

A produção de vidros temperados para protetores de tela tem despertado enorme interesse no crescente mercado de celulares, exigindo o uso de tecnologias para evitar fraturas durante a produção. O Método de Elementos Finitos (MEF) foi utilizado principalmente devido à sua eficácia e à possibilidade de simular modelos com geometrias complexas. Para atender ao maior número possível de aplicações, o material escolhido para a simulação foi o vidro *soda-lime*, vidro mais comumente produzido. A simulação da têmpera foi realizada no software Abaqus™ com sucesso utilizando a sub-rotina em Fortran UEXPAN para estimar os coeficientes de expansão térmica de cada elemento durante o resfriamento na faixa de transição vítrea. A análise do histórico de tensões durante a têmpera mostrou ser útil para evitar a fratura do material, uma vez que as tensões máximas de tração e compressão surgem muito antes da amostra atingir a temperatura ambiente. As tensões residuais no final da têmpera representam apenas cerca de 1-10% destas tensões máximas. A análise mostrou também que as tensões geradas dependem da geometria da amostra e a taxa de resfriamento. Além disso, observou-se que quanto maior for a relação superfície/volume, maior é a taxa de resfriamento crítica, na qual os limites mecânicos dos vidros são atingidos, e mais fácil é realizar a têmpera sem fraturar a amostra. No final, foi obtida uma taxa de resfriamento crítico de ~7 °C/s para a produção de protetores de tela de celular, sendo possível a têmpera ao ar (1-10 °C/s). Um aspecto interessante do trabalho foi a possibilidade de estudar visualmente, passo a passo, a evolução das tensões. Inicialmente, verificou-se uma maior contração térmica no exterior da amostra, seguida de uma maior contração térmica no interior, resultando no conhecido perfil de tensões de compressão na superfície e de tração no interior. Por fim, o modelo desenvolvido em elementos finitos, neste trabalho, mostrou boa representação qualitativa, exibindo alguns fenômenos previstos pela teoria, como a inversão de tensões durante têmpera, ou que ocorrem na prática, como as estrias de tensão em amostras volumosas. Assim, o MEF apresentou-se como uma ferramenta poderosa para a simulação da têmpera de vidros, sendo possível aprimorar o modelo incluindo o fenômeno de relaxação de tensões durante a transição vítrea e a variação da temperatura de transição vítrea em função da taxa de resfriamento.

Palavras-chave: Método de Elementos Finitos. Têmpera. Vidro.

ABSTRACT

The production of tempered glass for screen protectors has aroused enormous interest in the growing smartphone market, requiring the use of technologies to prevent fractures during production. The Finite Element Method (FEM) was used mainly because of its effectiveness and the possibility of simulating models with complex geometries. In order to cover as many applications as possible, the material chosen for the simulation was soda-lime glass, the most commonly produced glass. The tempering simulation was successfully performed in Abaqus™ software using the Fortran subroutine UEXPAN to estimate the thermal expansion coefficients of each element during cooling in the glass transition range. Analysis of the stress history during hardening proved useful in preventing the material from fracturing, since the maximum tensile and compressive stresses appear long before the sample reaches room temperature. Residual stresses at the end of hardening represent only around 1-10% of these maximum stresses. The analysis also showed that the stresses generated depend on the geometry of the sample and the cooling rate. Furthermore, it was observed that the higher the surface/volume ratio, the higher the critical cooling rate, at which the mechanical limits of the glass are reached, and the easier it is to perform tempering without fracturing the sample. In the end, it was possible to obtain a critical cooling rate of ~7 °C/s for the production of smartphone screen protectors, meaning that air-tempering is possible (1-10 °C/s). An interesting aspect of the work was the possibility of visually studying, step by step, the evolution of stresses. Initially, there was greater thermal contraction on the outside of the sample, followed by greater thermal contraction in the bulk, resulting in the well-known profile of compressive stresses on the surface and tensile stresses in the bulk. Finally, the finite element model developed in this work showed good qualitative representation, exhibiting some phenomena predicted by theory, such as the inversion of stresses during tempering, or that occur in practice, such as stress striations in voluminous samples. Thus, the FEM proved to be a powerful tool for simulating glass tempering, being possible to improve the model by including the phenomenon of stress relaxation during the glass transition phase and the variation of glass transition temperature as a function of cooling rate.

Keyword: Finite Element Method. Tempering. Glass.

LIST OF ILLUSTRATIONS

LIST OF TABLES

LIST OF ACRONYMS

Tg - Glass transition temperature

SCL - Supercooled liquids

FEM - Finite element method

CTE - Coefficient of thermal expansion

XS - solidified fraction of the material

LSC - Laboratório de Simulação Computacional

DEMa - Departamento de Engenharia de Materiais

3D - Three-dimensional

Smax - Maximum value of the principal stress

LIST OF SYMBOLS

Δ	Variation

TABLE OF CONTENTS

1 INTRODUCTION

Glass is a nonequilibrium, non-crystalline condensed state of matter that exhibits a glass transition. They are widely used because of their chemical stability, high hardness and impact resistance. However, there is one property that stands out when compared to other materials: transparency (HÖLAND & BEALL, 2019).

Affecting not only its function, but also the durability and price of the product itself, glass is recognized as one of the most significant components in smartphone screens. Representing 22% of user complaints, broken displays impact directly the smartphone market (CHOI et al., 2016). To exploit this growing market, technologies such as screen protection have been created to respond to this demand and, among the various materials, tempered glass is a strong candidate for its production (LIU, 2016).

Tempering involves rapidly cooling glass from its liquid state. At the end of tempering, the glass is obtained under a state of compression on the surface balanced by tensile forces in the bulk. Depending on the intensity of these stresses generated during cooling, the glass may fracture, mainly due to its low tensile strength. It is therefore important to estimate these stresses in order to avoid material failure.

Due to the complexity of the calculations that must be carried out to estimate these stresses, especially when considering complex geometries, it is extremely advantageous to use technologies that may numerically solve complex problems or problems without analytical solutions, such as simulations via Finite Element Method (FEM).

FEM is a numerical method for solving differential equations that is widely applied throughout the world. It distinguishes itself from other traditional methods because it solves problems of high geometric and physical complexity, with high efficiency, a solid theoretical basis and a wide range of applications (BATHE, 2008).

Hence, this work aims to answer the questions: would it be possible to accurately simulate glass tempering via the Finite Element Method?

2 THEORETICAL FUNDAMENTALS

2.1 GLASSES

There are organic, inorganic, metallic and polymeric materials. While the existence of metals and ceramics dates back almost 12,000 years, glassmaking dates back about half that time (DAVIS & ZANOTTO, 2017). In the early days of mankind, the rapid cooling of extrusive rocks produced natural glasses such as pearlite and obsidian. However, it was around 4,500 to 6,000 years ago, in ancient Egypt, that the first glass was created by human hands, the most likely use of which was as an ornament (VOGEL, 2013). In principle, it is possible to produce glass from any material, as long as it does not crystallize during cooling from its liquid state to the glass transition temperature (Tg).

According to Zanotto and Mauro:

> Glass is a nonequilibrium, non-crystalline condensed state of matter that exhibits a glass transition. The structure of glasses is similar to that of their parent supercooled liquids (SCL), and they spontaneously relax toward the SCL state. Their ultimate fate, in the limit of infinite time, is to crystallize (ZANOTTO and MAURO, JNCS 2017, p. 490).

The glass transition temperature (Tg) is not a characteristic of the material, but a kinetic phenomenon that depends directly on its cooling speed (VARSHNEYA, 2013). When the supercooled liquid reaches the Tg range, its structure freezes without crystallizing, becoming glass. If it remains in this range for long enough, intrinsic structural relaxation will occur, reorganizing its structure via translational movements. (ZANOTTO and MAURO, 2017). However, the crystallization time increases exponentially at temperatures significantly lower than Tg. The concept is illustrated in Figure 1.

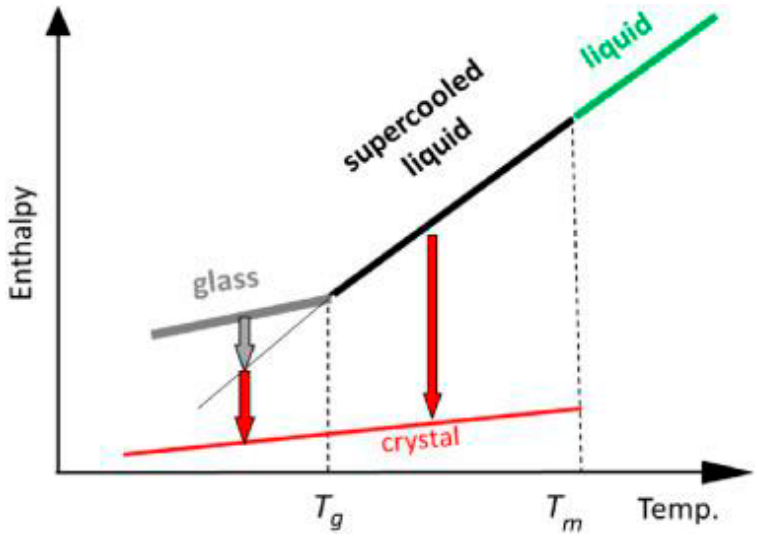

Figure 1 – Diagram of enthalpy versus temperature of vitreous materials (ZANOTTO and MAURO, 2017).

The long-range homogeneity of structure stands out among the many advantages of glass over other materials produced by mankind. This characteristic gives the material properties that come from the type of disorder in the chemical structure, such as good impact resistance, high hardness and transparency (HÖLAND & BEALL, 2019).

Seeking to serve as many applications as possible, the focus of this work will be on **soda-lime glass** in particular, most common form of glass produced.

2.2 SMARTPHONE SCREEN PROTECTORS

Affecting not only its function, but also the durability and price of the product itself, glass is recognized as one of the most significant components in smartphone screens. Characteristics such as mechanical strength, flexibility and thickness summarize the focus found in today's display industry (CHOI et al., 2016).

In 2013, the main complaint on smartphone customer service was screen breakage, with a proportion of 22%, as shown in Figure 2. This assessment shows that hardware damage is more significant to the consumer than the communication function itself, even for smartphones (CHOI et al., 2016).

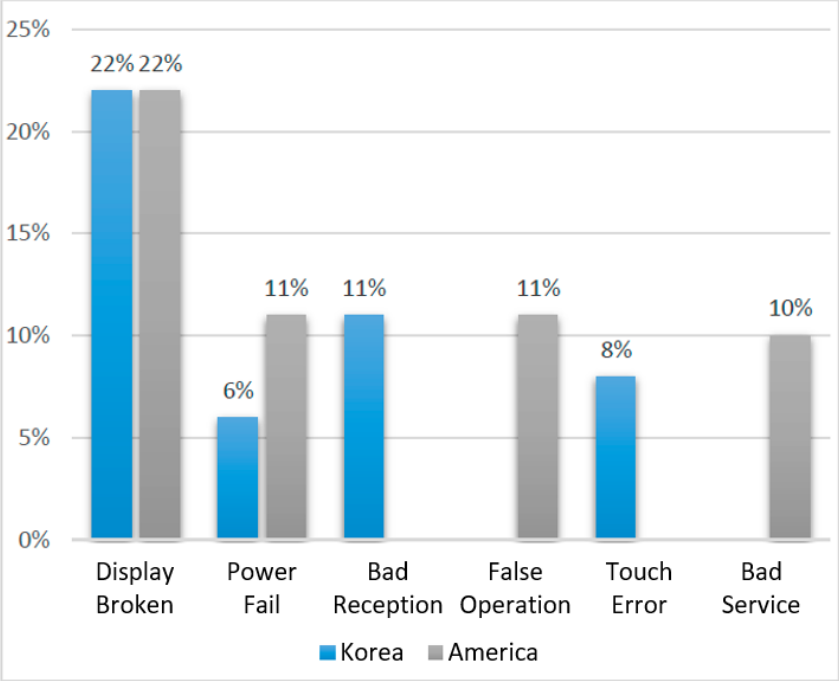

Figure 2 – Main reasons for smartphone customer service complaints. Adapted from (CHOI et al., 2016).

The cell phone market is growing rapidly, increasing from 1157.2 to 1848.6 million units sold worldwide between 2009 and 2014, *i.e.*, a growth of 63% in only 5 years. This market therefore represents the number of units of glass screens used (TELECO, 2014).

Gorilla Glass is an example of product that fits into this market. This technology, based on ion exchange (surface replacement of smaller ions by larger ones), is present in around 1000 types of devices from 33 companies and has been found in more than 1 billion electronic devices in the last 6 years (GUIGLIELMO, 2013).

Given that the smartphone screen market remains promising, the development of screen protections can be extremely advantageous. In this market, tempered glass screen protectors have shown better sensitivity to finger touch and quicker response of a smartphone's interface when compared to competing screen protectors: Anti-Smudge, Anti-Smudge and Glare and Blue Light Cut (LIU, 2016).

Therefore, this work will discuss the use of tempered glass for **screen protectors** manufacturing.

2.3 TEMPERED GLASSES

Tempering involves rapidly cooling glass from its liquid state. Once in contact with the environment (air or water), the surface of the glass cools more quickly than the bulk, creating a temperature gradient between the surface and the bulk. Initially, the thermal contraction of the surface is greater than that of the bulk, producing tensile stresses on the surface and compressive stresses internally. The bulk then cools more quickly than the surface, until isothermal conditions are established at room temperature. At this point, the thermal contraction of the bulk exceeds that of the surface, producing tensile stresses in the bulk and compressive stresses on the surface (GARDON, 1980).

If the material were an elastic solid, the opposing stresses would be canceled out. However, as previously mentioned, glass exhibits the phenomenon of structural relaxation when subjected to high temperatures. Thus, most of the stresses induced initially are relaxed because the glass is still hot, and most of the stresses induced at the end of solidification remain (NARAYANASWAMY & GARDON, 1969).

At the end of tempering, the glass is obtained under a state of compression on the surface balanced by tensile forces in the bulk. Depending on the intensity of these stresses generated during cooling, the glass may fracture, mainly due to its low tensile strength. It is therefore important to estimate these stresses in order to avoid material failure during processing.

The mathematical estimation of residual stresses in tempered glass requires a simultaneous analysis of the glass's thermal history and its mechanical response. A possible simplification of a glass's rheological behavior under tempering is that of "instantaneous freezing" at Tg, disregarding all complex phenomena that occur in the glass transition range. It is assumed that, above Tg, the glass behaves like a fluid incapable of accumulating shear stresses and, below Tg, it behaves like an elastic solid (BARTENEV, 1949).

However, this simplification does not cover the transient stresses observed experimentally during glass cooling and is therefore not suitable when a glass is cooled from high temperatures to Tg. To complement the analysis, the glass relaxation

in the glass transition range must be considered (LEE et al., 1965).

Due to the complexity of the calculations that must be carried out, especially when needing to consider the 3D geometry of the samples, it is extremely advantageous to use technologies that optimize these calculations, such as simulation software using **Finite Element Method**.

2.4 FINITE ELEMENT METHOD

The Finite Element Method (FEM) is a modern and sophisticated numerical method for solving differential equations, widely applied in the field of elastic structures. Its mathematical principle is simple. It is well known that a large round pool can be built with small rectangular bricks. The smaller the bricks, the closer the pool is to a perfect circumference. Similarly, FEM is mathematically based on the variational principle and the subdivision approximation, *i.e.*, the finer the subdivision, the greater the approximation. Complex geometries can be divided into a finite number of fundamental elements (points, lines, areas and volume elements). To determine a function that extends over the entire geometry, a piecewise interpolation is performed, which is usually a simple linear interpolation or a low-order polynomial. As a result, a quadratic function problem with infinite degrees of freedom becomes just a system of linear algebraic equations, which allows the function of global energy to be approximated by a sum of the energies of these finite elements (BATHE, 2008).

FEM stands out from other traditional methods because it solves problems with high geometric and physical complexity, with high efficiency, a solid theoretical basis and a wide range of applications. Therefore, it was the method chosen to model glass tempering in this work. If the radiating effects are ignored, calculating the temperatures and thermoelastic stresses in the glass is simple. The biggest problem is estimating the thermal relaxation and contraction phenomenon when the glass is in the Tg range.

To counter this limitation, a simplification was established in this work where the material would follow the behavior of a mixture of liquid and solid phases, respectively, between the start and end temperatures of the glass transition, with properties intermediate to its liquid and glassy form. From Equations 1 and 2, it is

possible to calculate the Coefficient of Thermal Expansion (CTE) for each element in the sample as a function of the solidified fraction of the material (XS) and the node temperature (T).

$$XS = \frac{Tg_i - T}{Tg_i - Tg_e} \quad ; \quad Tg_e < T < Tg_i \quad ; \quad 0 < XS < 1 \qquad Equation\ 1$$

$$CTE = XS * CTE_e + (1 - XS) * CTE_i \quad ; \quad CTE_e < CTE < CTE_i \qquad Equation\ 2$$

Where Tg_i and Tg_e are the initial and end temperatures of the glass transition, respectively. CTE_i and CTE_e are the thermal expansion coefficients of the liquid and glass phases, respectively.

3 MATERIALS AND METHODS

3.1 SODA-LIME GLASS PROPERTIES

All the general properties of soda-lime glass were obtained from CES 2019 Edupack, a database tool for material selection, while the CTE at high temperatures was obtained from Gottsmann's study. These properties are shown in Table 1 and their values were used as inputs for the FEM analysis.

Table 1 – Soda-lime glass properties used as inputs on the FEM analysis.

Property	Mean Values (CES 2019 Edupack)
Composition	73 w.% SiO2, 1 w.% Al2O3, 17 w.% Na2O, 4 w.% MgO, 5 w.% CaO
Density	2460 kg/m^3
Young's modulus	70 GPa
Poisson's ratio	0.215
Tensile strength	33 MPa
Compressive strength	326 MPa
Specific heat capacity	900 J/(kg.°C)
Initial Temperature of Glass Transition (Tg_i)	592 °C
CTE at 640 °C (GOTTSMANN, 1999)	88.1 µstrain/°C
End Temperature of Glass Transition (Tg_e)	442 °C
CTE below Tge	9.345 µstrain/°C

3.2 FEM MODELS

3.2.1 Finite Element Software

All the FEM modeling was carried out on the software ABAQUS/CAE 6.14-1, provided by the Laboratório de Simulação Computacional (LSC), from portuguese *Computational Simulation Laboratory*, of the Departamento de Engenharia de Materiais (DEMa), from portuguese *Materials Engineering Department*.

3.2.2 Analysis Sub-Routine

In order for the analysis to incorporate the phenomenon when the glass enters the glass transition range, a Fortran UEXPAN subroutine was written to include Equations 1 and 2 as discussed in 2.4 FINITE ELEMENT METHOD. The complete code used in the subroutine is shown in Appendix A.

3.2.3 Cylinder's Cross-section - axisymmetric

A cylinder cross-section was chosen to be the first model, due to its simple geometry, with a height significantly greater than the thickness of smartphone screen protectors. Figure 3 shows its dimensions (20 x 20 mm), with a Y-axis radial symmetry, analyzing **only half** of the cross-section (10 x 20 mm).

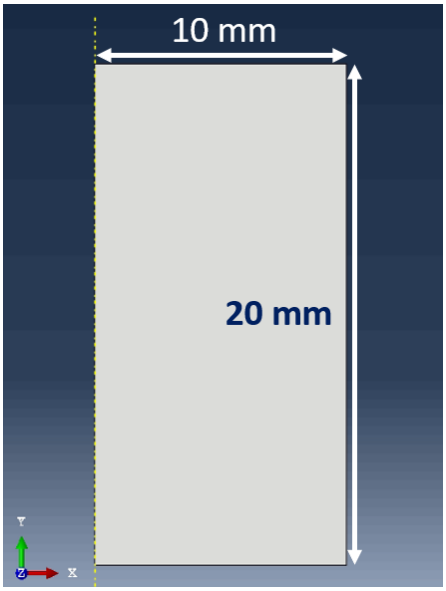

Figure 3 – Axisymmetric modeling of cylinder's half cross-section.

3.2.4 Disc's Cross-section - Axisymmetric

The same was done for the disc modeling, using the average dimensions of smartphone screen protectors. As shown in Figure 4, its dimensions are 164 x 2 mm, with a Y-axis radial symmetry, analyzing **only half** of the cross-section (82 x 2 mm).

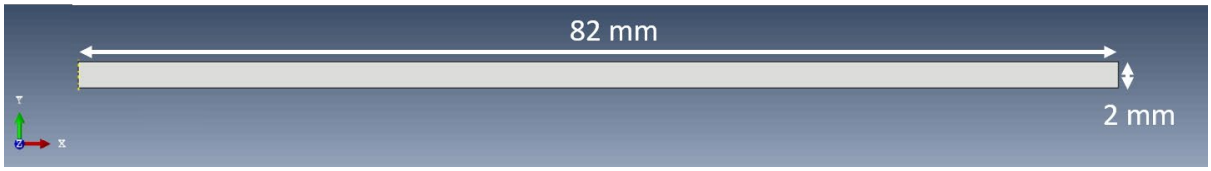

Figure 4 – Axisymmetric modeling of disc's half cross-section.

3.2.5 Smartphone Screen Protector - 3D

Finally, the smartphone screen protector 3D model was done, also using the average dimensions of smartphone screens. As shown in Figure 5, its dimensions are 164 x 76 x 2 mm, with XZ and YZ planes symmetry, analyzing **only 1/4** of the sample (82 x 38 x 2 mm).

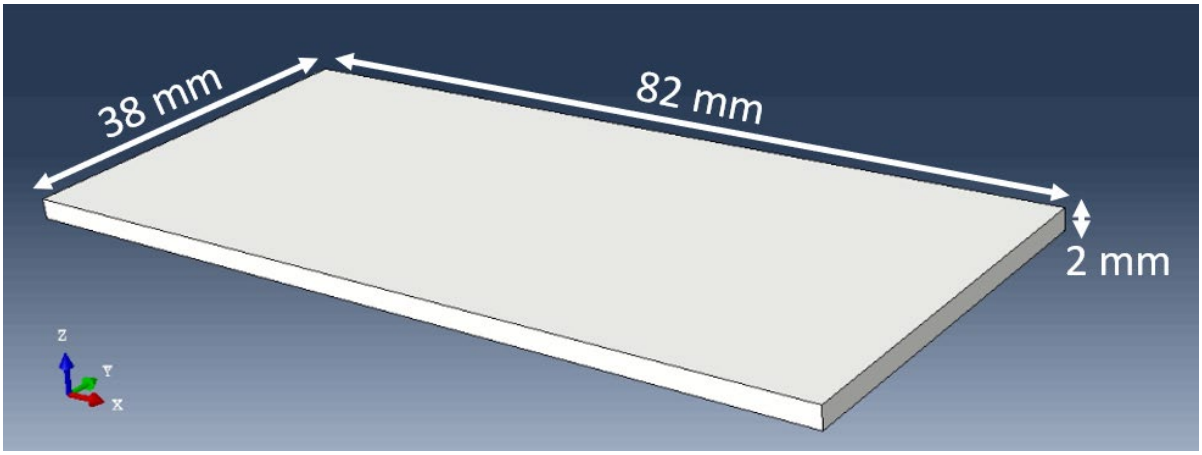

Figure 5 – 3D modeling of 1/4 smartphone screen protector.

3.2.6 Boundary Conditions

To ensure symmetry, a zero x-shift was imposed on the construction line represented in yellow, as well as an initial temperature throughout all the nodes of the model. Cooling was applied as a direct reduction of temperature on the surfaces, represented in red, with no direct exchange of heat between the sample and the environment, only between its hot bulk and its cold surface. The cooling follows the temperature and time values contained in the associated amplitude table, making it possible to determine the exact cooling rate for each case. The boundary conditions described above are shown in figures 6 to 8.

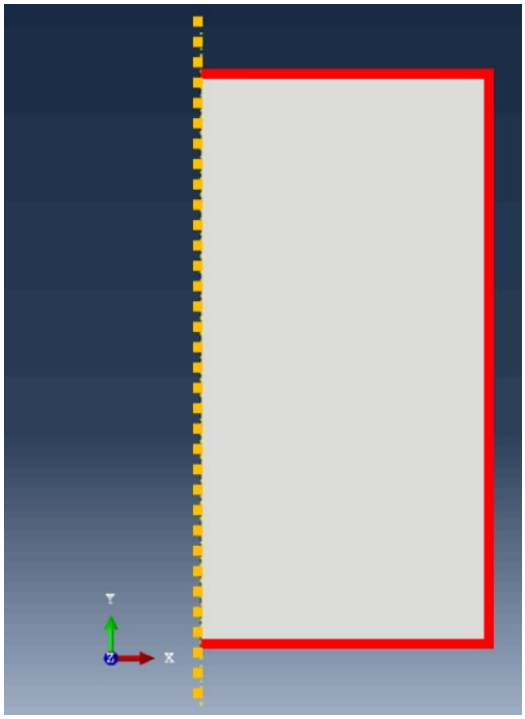

Figure 6 – Boundary conditions on axisymmetric model of the cylinder's half cross-section.

Figure 7 – Boundary conditions on axisymmetric model of the disc's half cross-section.

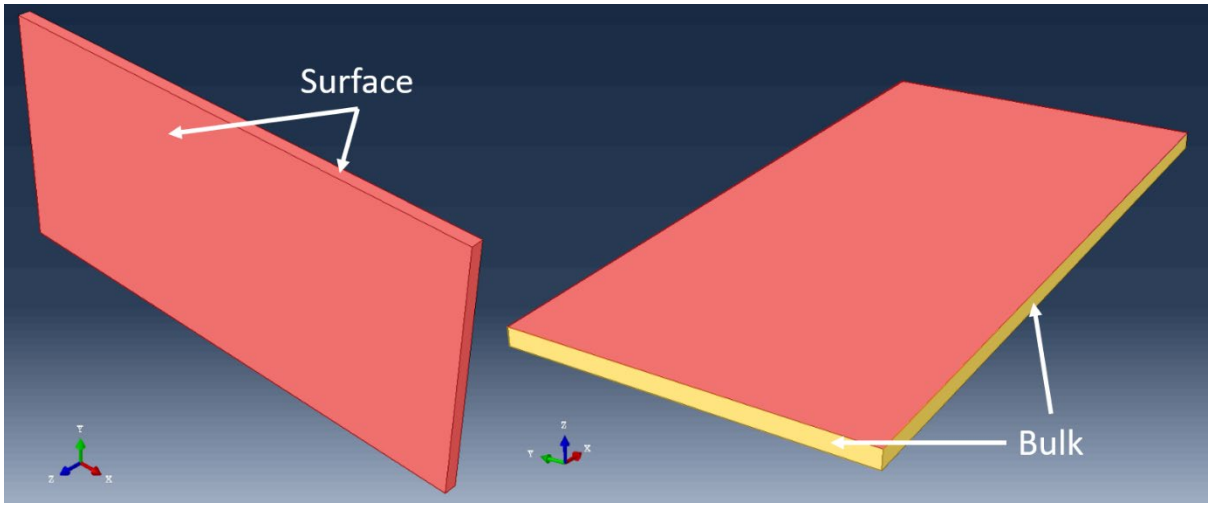

Figure 8 – Boundary conditions on 3D model of the 1/4 smartphone screen protector.

The initial condition was kept the same for all the models, going from 800 °C to 25 °C in 10 seconds, equivalent to a cooling rate of 77.5 °C/s. In this condition, it was possible to study the stress evolution during tempering and the difference in results depending on the geometry of the samples and between axisymmetric and 3D analyses.

To analyze the effect of cooling rate, a finite element analysis was performed on each model in order to find an equilibrium cooling condition. This second condition was obtained by reducing the cooling rate in each model until the maximum and minimum stresses were confined within the tensile and compressive strength range of the soda-lime glass. Under these conditions, it was possible to study not only the effect of the cooling rate on the intensity of the hardening stresses, but also how this effect becomes more or less significant for some specific geometries. At the end, these equilibrium conditions represent the critical cooling rate for each soda-lime glass sample not to fracture under tempering treatments.

3.3 MESH CONVERGENCE ANALYSIS

Before starting all the analyses, it was necessary to ensure that the simulations were consistent. If the mesh element size was too small, the accuracy of the analysis would be high, but the computational calculations to obtain results would be too long. If the element mesh size was too large, the calculation would diverge from reality.

Therefore, in order to find a reasonable mesh, a convergence study was carried out on all the sample models.

To optimize the calculation time and also the accuracy of the numerical simulation, a number of mesh elements close to the convergence asymptote was chosen. This required comparing the evolution of values of a defined variable by performing several analyses with different numbers of mesh elements. As glass is more fragile to tensile stress than compressive stress, it was desirable for the value to be converged in this stress field. Therefore, the variable chosen was the maximum positive value of the principal stress (Smax) at the end of the tempering.

The type of mesh element was chosen in a standard element library with a linear geometric order. For the axisymmetric model, the mesh element type was CAX4T: a 4-node axisymmetric thermally coupled quadrilateral, bilinear displacement and temperature, structured with a quadrilateral-dominated element shape. For the tridimensional model, the mesh element type was C3D8T: an 8-node thermally coupled brick, trilinear displacement and temperature, structured with a hexahedron element shape.

It was defined that the convergence criterion would be reached when Equation 3 was satisfied.

$$\frac{|Smax_n - Smax_{n-1}|}{Smax_{n-1}} = \frac{|\Delta Smax_n|}{Smax_{n-1}} \leq 0{,}3\% \qquad Equation\ 3$$

Despite being used for mesh convergence, the stress values at the end of the analysis do not represent the critical values to which the material will be subjected. Therefore, in order to be able to predict whether the material would fracture, the analysis was carried out looking to the global maximum and minimum values throughout the simulation.

3.4 CHAMFERING/ROUNDING ANALYSIS

There is a complex interaction of forces and moments at the corners of the samples, leading to a concentration of stresses due to the abrupt transition of

geometry in these regions. Chamfering/rounding are techniques designed to reduce the angle of edges or vertices formed by the meeting of faces perpendicular to each other, thus promoting a more uniform distribution of stresses and minimizing the points of maximum stresses at the corners.

Therefore, after converging the meshes of each model, samples were created with chamfered and rounded corners in order to analyze the effect on the stress history generated during tempering.

3.4.1 Chamfering/Rounding on Cylinder's Half Cross-section - axisymmetric

Since there is radial symmetry in the cylinder cross-section model, any slice in its plane shows the bulk and the external corners of the sample, allowing analysis to be performed on the simplest axisymmetric models.

Figure 9 shows the models with their chamfered and rounded corners. The chamfering was done by creating a simple line between points A and B, while the rounding was done by creating a curve that tangents both edges of the model. The boundary conditions remain the same as previously described in 3.2.6 BOUNDARY CONDITIONS, where the lines in yellow and red represent, respectively, the axis of symmetry (internal side) and the cooled surfaces (external side).

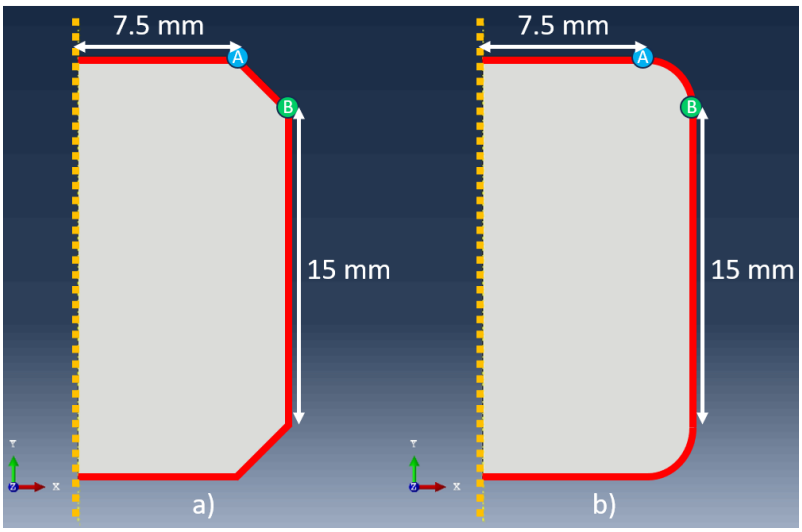

Figure 9 – axisymmetric models of cylinder's half cross-section with a) chamfering and b) rounding.

3.4.2 Chamfering/Rounding on Smartphone Screen Protector - 3D

Because there is no radial symmetry in the screen protection model, the cross-section represents a slice of the glass plane middle, limiting the analysis to the more complex 3D model.

Figure 10 shows the models with their chamfered and rounded corners, obtained the same way as before, under the same boundary conditions, where yellow and red areas represent, respectively, the symmetry surface (in bulk) and the cooled surfaces (external side).

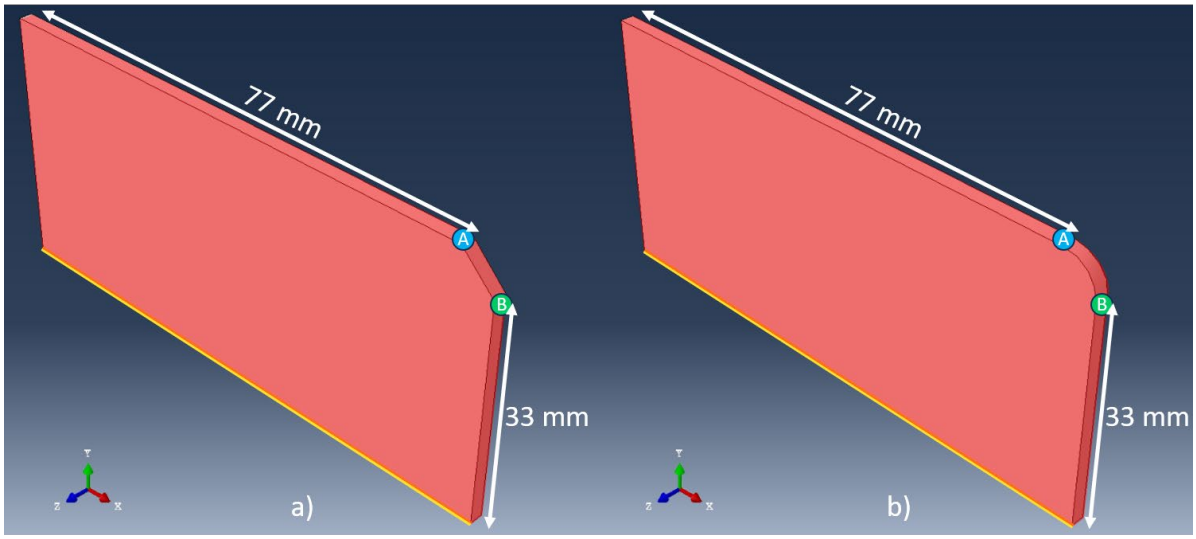

Figure 10 – 3D models of 1/4 smartphone screen protector with a) chamfering and b) rounding.

4 RESULTS

4.1 MESH CONVERGENCE

The results of 3.3 MESH CONVERGENCE ANALYSIS are presented below.

4.1.1 Mesh Convergence on Cylinder Cross-section - Axisymmetric

Table 2 – Data obtained from the mesh convergence analysis on the axisymmetric model of the cylinder's half cross-section.

Cylinder's half cross-section - Axisymmetric		
Number of mesh elements	Smax [MPa]	$\lvert\Delta Smax_n/Smax_{n-1}\rvert$ [%]
50	52.980	-
91	8.197	84.53
200	5.783	29.45
325	5.949	2.87
561	5.904	0.76
648	5.858	0.78
800	**5.869**	**0.19**
1250	5.857	0.20
5000	5.852	0.09

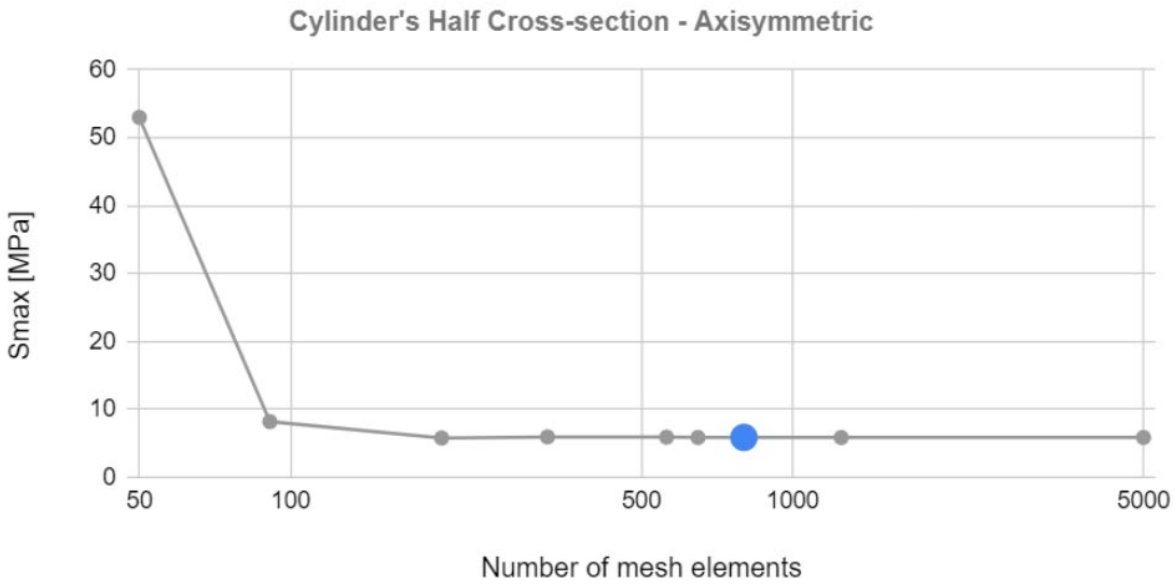

Figure 11 – Mesh convergence graph on the axisymmetric model of the cylinder's half cross-section.

Table 2 and Figure 11 show that it was possible to converge the results, according to the criterion of $\lvert\Delta Smax_n/Smax_{n-1}\rvert < 0.3\%$, with 800 mesh elements, making it possible to proceed with the simulations.

4.1.2 Mesh Convergence on Disc Cross-section - Axisymmetric

Table 3 – Data obtained from the mesh convergence analysis on the axisymmetric model of the disc's half cross-section.

Disc's half cross-section - Axisymmetric		
Number of mesh elements	Smax [MPa]	|ΔS/S0| [%]
50	0.2485	-
200	0.3706	49.13
300	0.4898	32.16
400	0.5424	10.74
800	0.5292	2.43
1000	0.5231	1.15
1200	**0.5220**	**0.21**
5000	0.5211	0.17

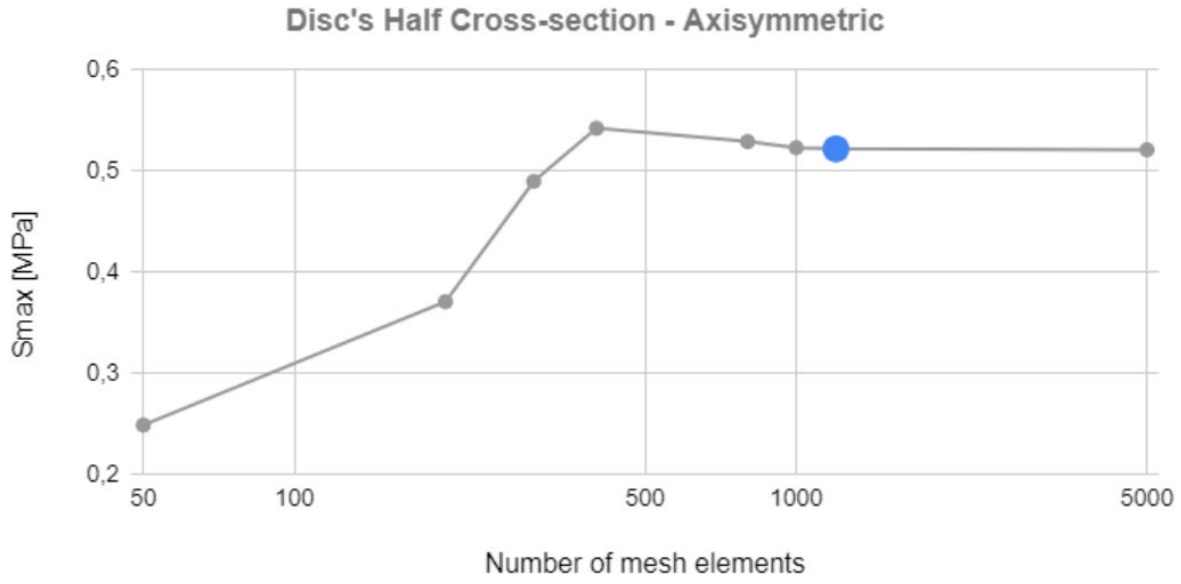

Figure 12 – Mesh convergence graph on the axisymmetric model of the disc's half cross-section.

Table 3 and Figure 12 show that it was possible to converge the results, according to the criterion of $|\Delta Smax_n/Smax_{n-1}| < 0.3\%$, with 1200 mesh elements, making it possible to proceed with the simulations. The increase in the number of elements required is probably due to the larger dimensions of the mesh compared to half the cross-section of the cylinder.

4.1.3 Mesh Convergence on Smartphone Screen Protector - 3D

Table 4 – Data obtained from the mesh convergence analysis on the 3D model of the 1/4 smartphone screen protector.

1/4 Smartphone Screen Protector - 3D		
Number of mesh elements	Smax [MPa]	|ΔS/S0| [%]
500	0.8856	-
1000	0.7497	15.35
1440	0.6681	10.88
1690	0.7295	9.19
1960	0.7112	2.51
2250	0.7057	0.77
2560	**0.7077**	**0.28**
5000	0.7089	0.17

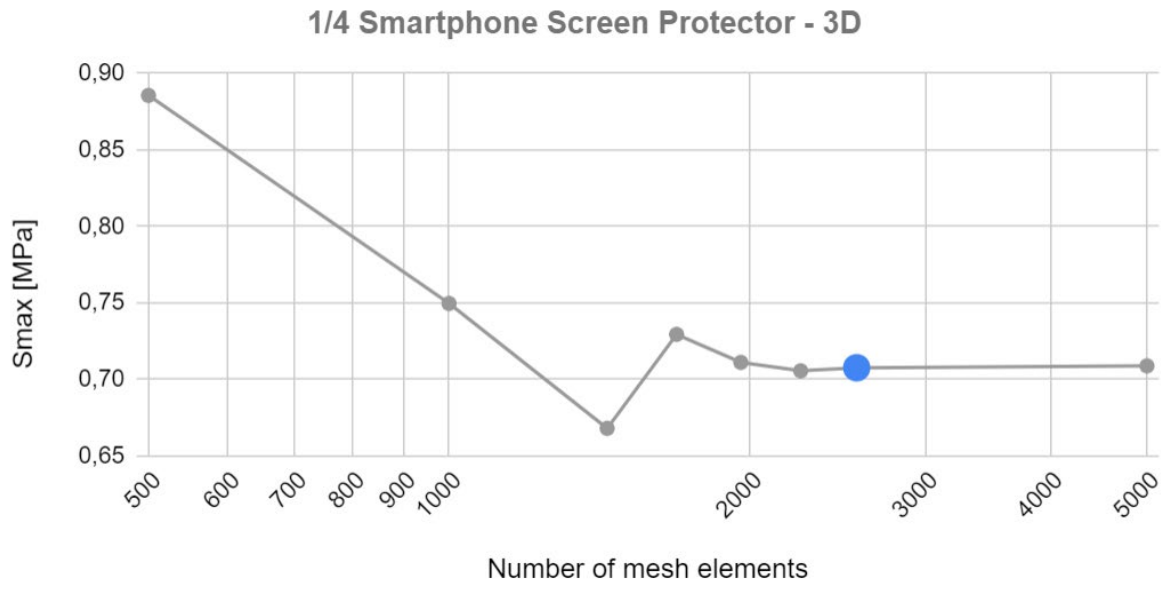

Figure 13 – Mesh convergence graph on the 3D model of the 1/4 smartphone screen protector.

Table 4 and Figure 13 show that it was possible to converge the results, according to the criterion of $|\Delta Smax_n/Smax_{n-1}| < 0.3\%$, with 2560 mesh elements, making it possible to proceed with the simulations. As this is a three-dimensional model, the number of elements required is expected to be even higher.

4.2 STRESS SIMULATION

The results of 3.2 FEM MODELS stress simulation analysis are presented below. As explained previously, the initial condition of the stress simulation was a cooling rate of 77.5 °C/s and was only varied in 4.4 EFFECT OF COOLING RATE.

4.2.1 Effect of Geometry

Figures 14 and 15 show, respectively, the instants during simulation when the maximum principal stresses reached their maximum and final values (at the end of the simulation) in the axisymmsetric model of the cylinder's half cross-section. The values are compared in Table 5.

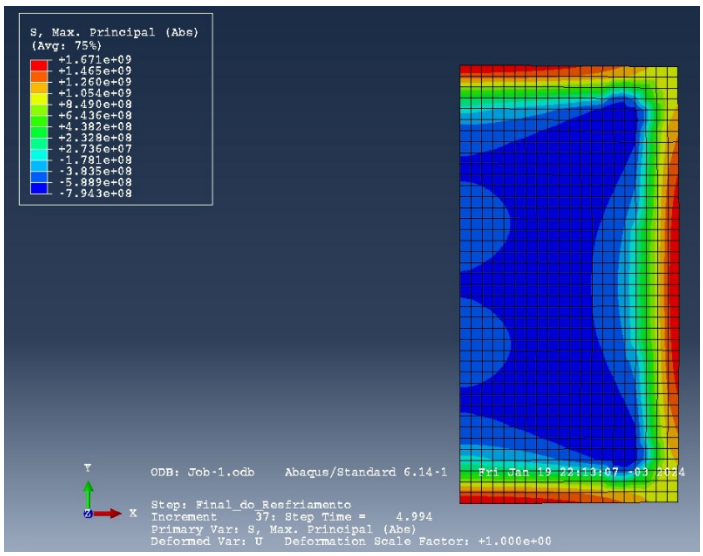

Figure 14 – Simulation step where the stresses reached their maximum values in the axisymmetric model of the cylinder's half cross-section.

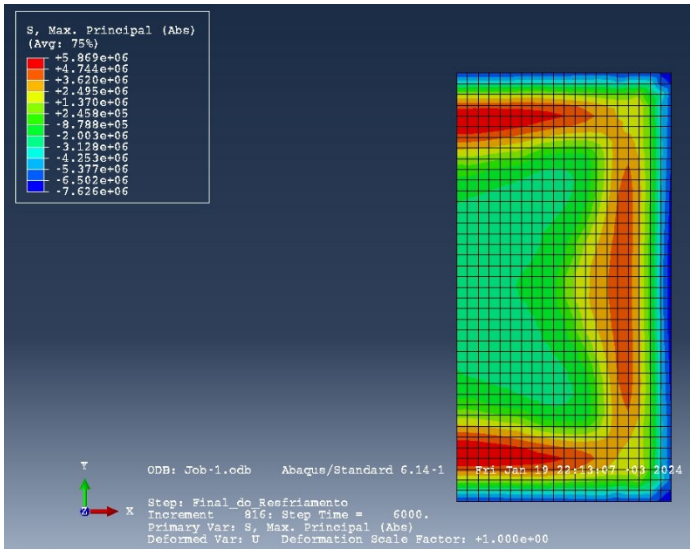

Figure 15 – Simulation last step where the stresses reached their final values in the axisymmetric model of the cylinder's half cross-section.

Figures 16 and 17 show, respectively, the moments in the simulation when the stresses reached their maximum and final values (at the end of the simulation) in the axisymmetric model of the disc's half cross-section. The values are compared in Table 5.

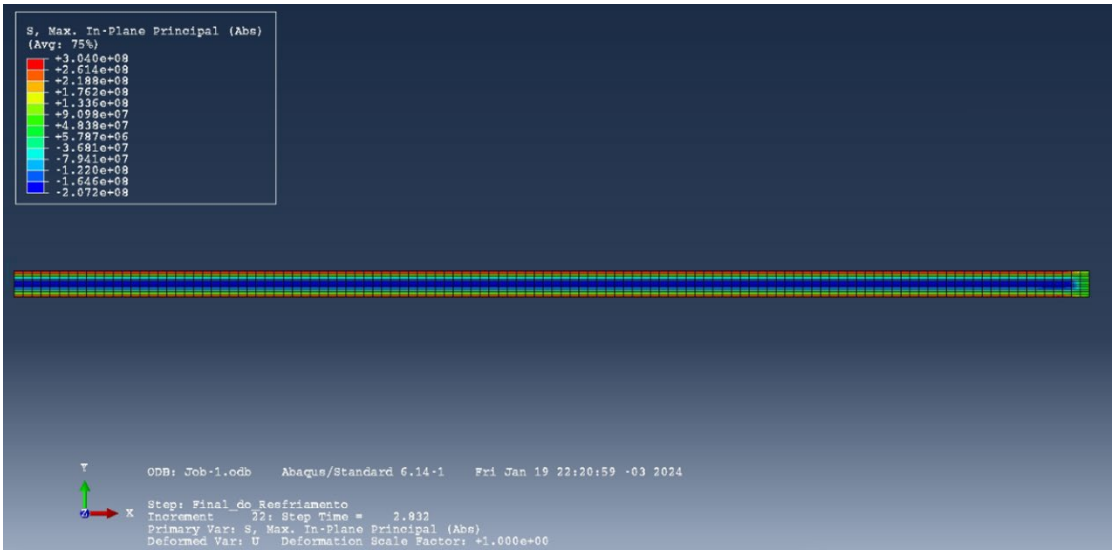

Figure 16 – Simulation step where the stresses reached their maximum values in the axisymmetric model of the disc's half cross-section.

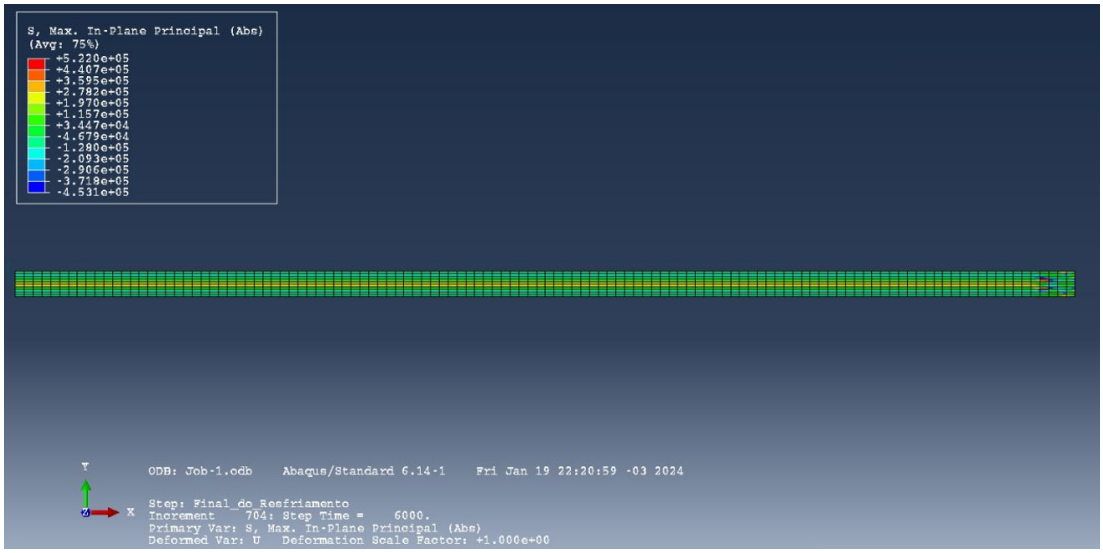

Figure 17 – Simulation last step where the stresses reached their final values in the axisymmetric model of the disc's half cross-section.

Table 5 – Values obtained by the geometry analysis, represented in red or green when, respectively, above or below the mechanical strength of the soda-lime glass.

Cooling Rate: 77.5 °C/s	Axisymmetric Cylinder [MPa]	Axisymmetric Disc [MPa]	Mechanical Strength [MPa]
Maximum Tensile Stress	1671	304	33
Maximum Compression Stress	1372	208	326
Final Tensile Stress	6	0.5	33
Final Compression Stress	8	0.4	326

As the red fields in Table 5 show, both models have iterations where the stress exceeds the strength of the material, leading to fracture, while the green fields represent the stresses within the material's entire mechanical strength range. However, it can be seen that the stress values in the cylinder model exceed those of the screen by 1 order of magnitude. This is probably because the cylinder has a large internal volume, increasing the temperature gradient between its bulk portion and the surface, which results in high stresses. However, the disc/screen protector has a much smaller thickness than its length, generating a reduced stress gradient.

4.2.2 Comparison of axisymmetric and 3D Simulations

Figures 18 and 19 show, respectively, the instants during simulation when the stresses reached their maximum and final values (at the end of the simulation) in the 3D model of the 1/4 smartphone screen protector. The values are shown in Table 6.

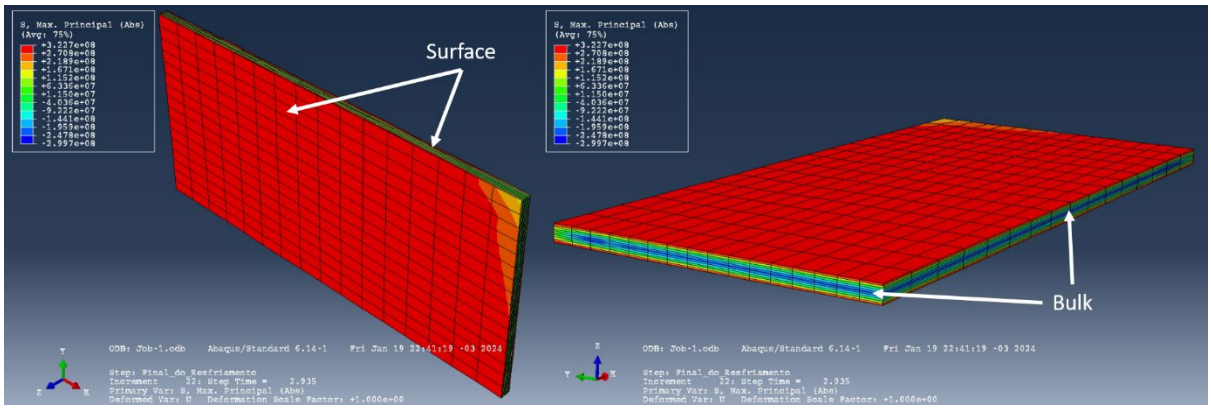

Figure 18 – Simulation step where the stresses reached their maximum values in the 3D model of the 1/4 smartphone screen protector.

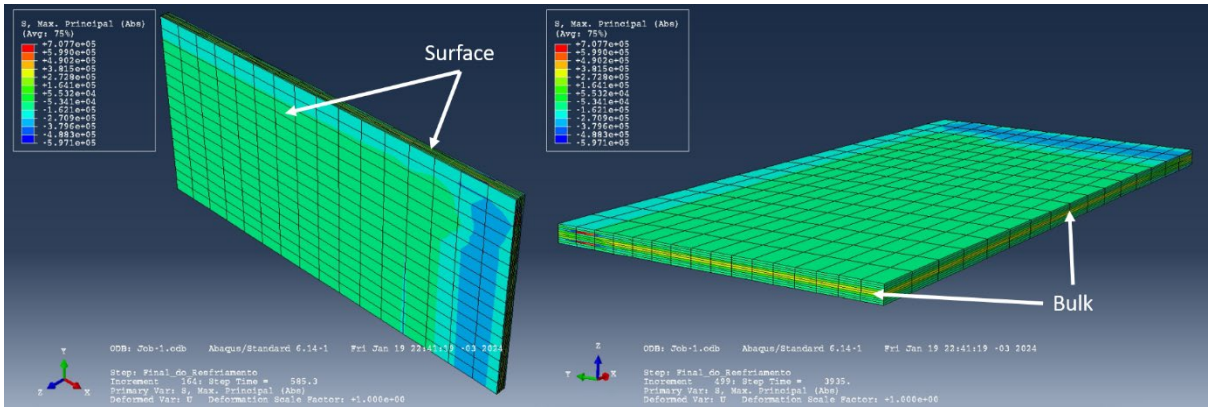

Figure 19 – Simulation step where the stresses reached their final values in the 3D model of the 1/4 smartphone screen protector.

Table 6 – Values obtained by the axisymmetric x 3D analysis, represented in red or green when, respectively, above or below the mechanical strength of the soda-lime glass.

Cooling Rate: 77.5 °C	Axisymmetric Disc [MPa]	3D Screen [MPa]	Mechanical Strength [MPa]
Maximum Tensile Stress	304	323	33
Maximum Compression Stress	208	300	326
Final Tensile Stress	0.5	0.7	33
Final Compression Stress	0.4	0.6	326

It is noticeable that all the stresses measured in the three-dimensional model exceed the stress values calculated in the axisymmetric model. The reason for this might be that, in the axisymmetric model, the software only considers the heat exchange between adjacent elements within the same plane, and does not consider the interaction between elements in adjacent planes. Furthermore, the 3D model shows that stresses vary across the volume, so each cross-section would have a different stress profile depending on the distance to the outer edges.

4.2.3 Stress Evolution During the Tempering

The stress evolution during the tempering simulation was entirely analyzed on the 3D model of 1/4 smartphone screen protector, shown below in figures 20 to 25. These figures represent the consecutive increment of the analysis during the moment of stress inversion, except for Figure 25, which shows the final state of stresses.

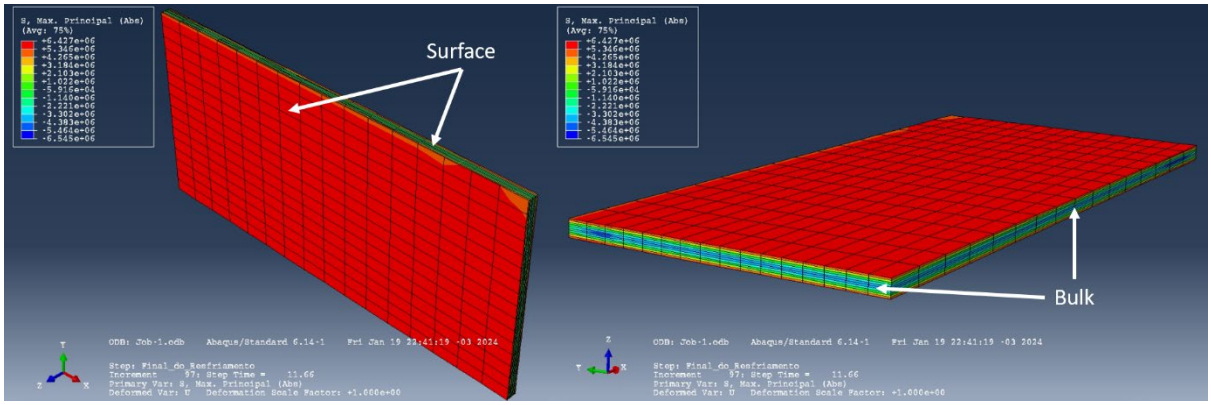

Figure 20 – Increment 97 of the simulation. Tensile (red > orange > yellow) and compressive (blue > green) stresses can be seen.

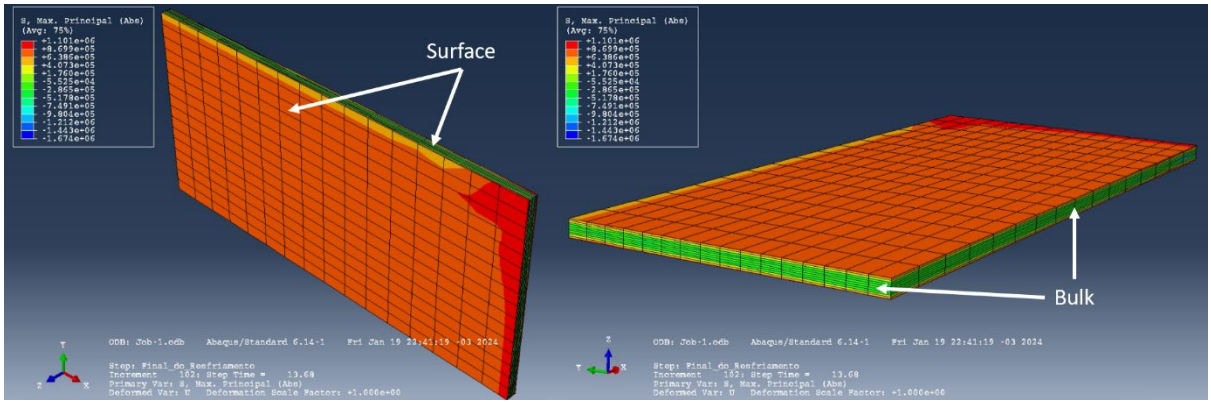

Figure 21 – Increment 102 of the simulation. Tensile (red > orange > yellow) and compressive (green) stresses can be seen.

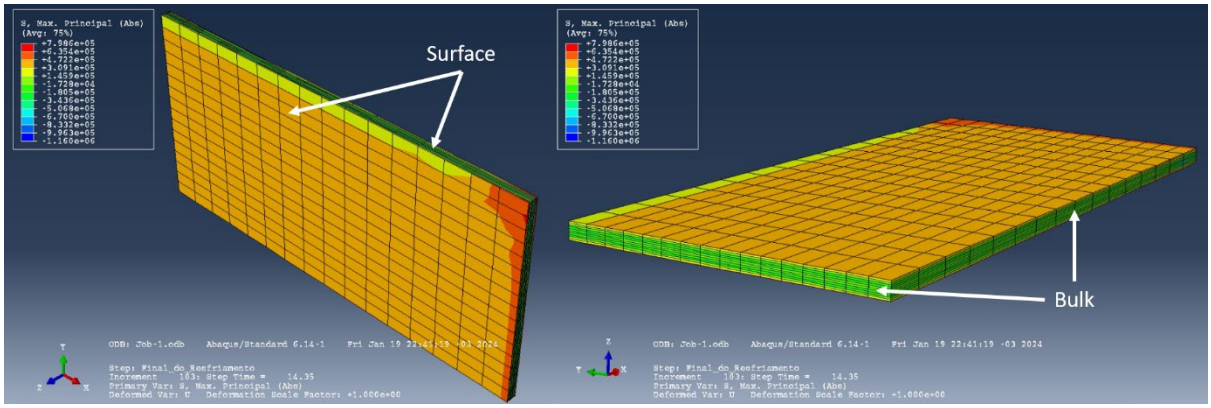

Figure 22 – Increment 103 of the simulation. Tensile (red > orange > yellow) and compressive (green) stresses can be seen.

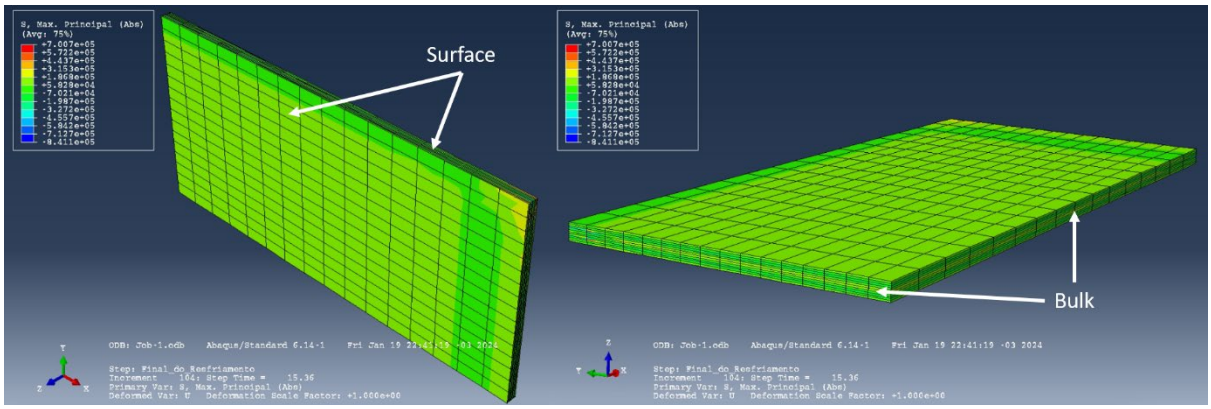

Figure 23 – Increment 104 of the simulation. Tensile and compressive stresses are close to zero (green).

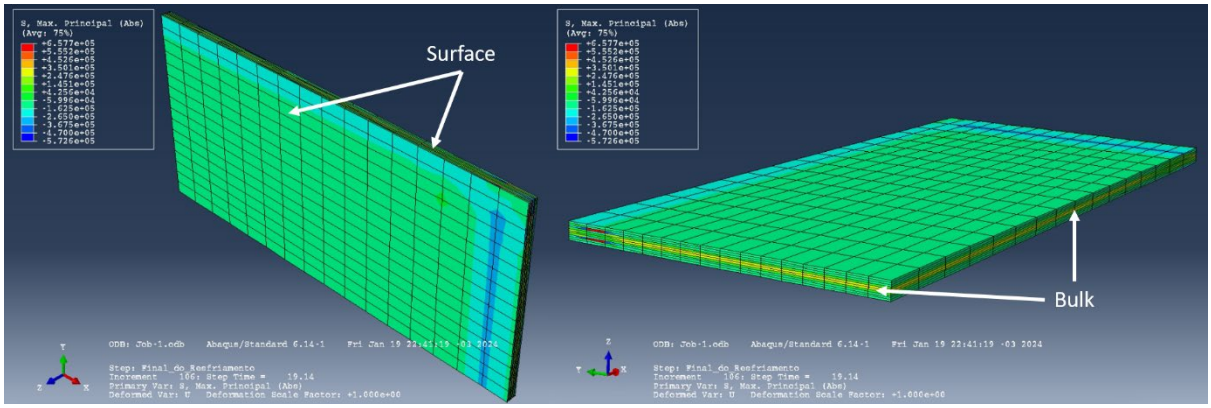

Figure 24 – Increment 106 of the simulation. Tensile (red > orange > yellow) and compressive (blue > green) stresses can be seen.

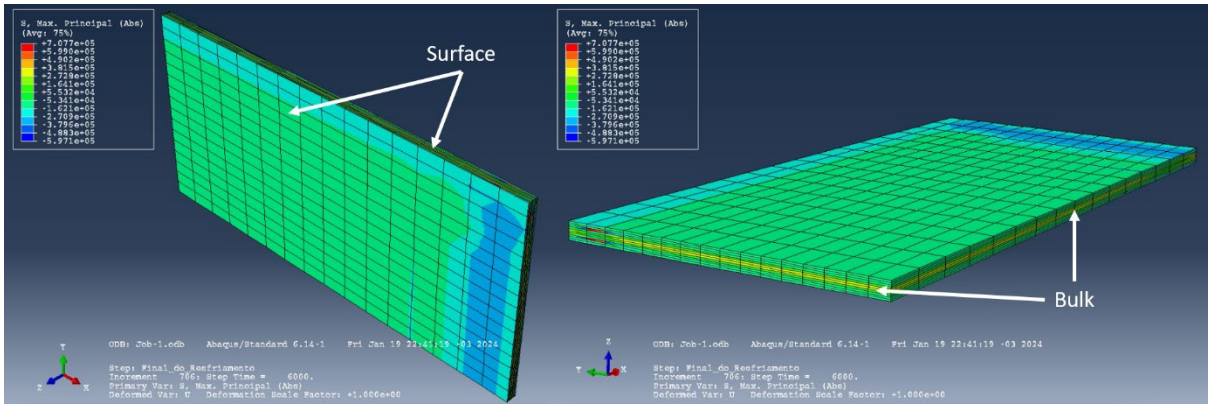

Figure 25 – Increment 706 of the simulation. Tensile (red > orange > yellow) and compressive (blue > light blue > green) stresses can be seen.

Initially, there is tensile stress on the surface (red, orange, yellow) and compression stress in the bulk (green), as shown in Figure 20. In Figure 21, the tensile and compressive stress reduces a little, with a greater reduction at the corners than on the surface. In Figure 22, the tensile stress reduces drastically, mostly at the corners. In Figure 23, the compression from the inside spreads through the entire sample, and the stresses roughly cancel each other out. Figure 24 shows a complete inversion of the stresses on the surface, going from traction to compression. This also occurs in the bulk, going from compression to traction. Finally, Figure 25 shows the state of stress at the end of the simulation, with compression on the surface (especially intense at the corners) and a tensile profile on the inside.

The evolution of stresses in the simulation is qualitatively in agreement with the theoretical prediction. Initially, there was tensile stress on the surface and compressive one in the bulk followed by an inversion of stresses due to the cooling of the liquid bulk, reaching a final state of compression on the surface and traction in the bulk portion. It was even possible to see the moment when the stresses cancel each other out before the inversion.

It is worth noting that although the simulation is correct qualitatively, it is not possible to say that it is correct quantitatively, as the model does not predict stress relaxation phenomena in the liquid phase or Tg variation as a function of the cooling rate in each node. These simplifications may be corrected during model improvement in future works.

4.3 EFFECT OF CHAMFERING/ROUNDING

The results of 3.4 CHAMFERING/ROUNDING ANALYSIS are presented below.

4.3.1 Effect of Chamfering/Rounding on Cylinder's Half Cross-Section - Axisymmetric

Figures 26 and 27 show, respectively, the instants during simulation when the stresses reached their maximum and final values (at the end of the simulation) in the axisymmetric model of the cylinder's half cross-section with chamfering/rounding. The values are compared in Table 7.

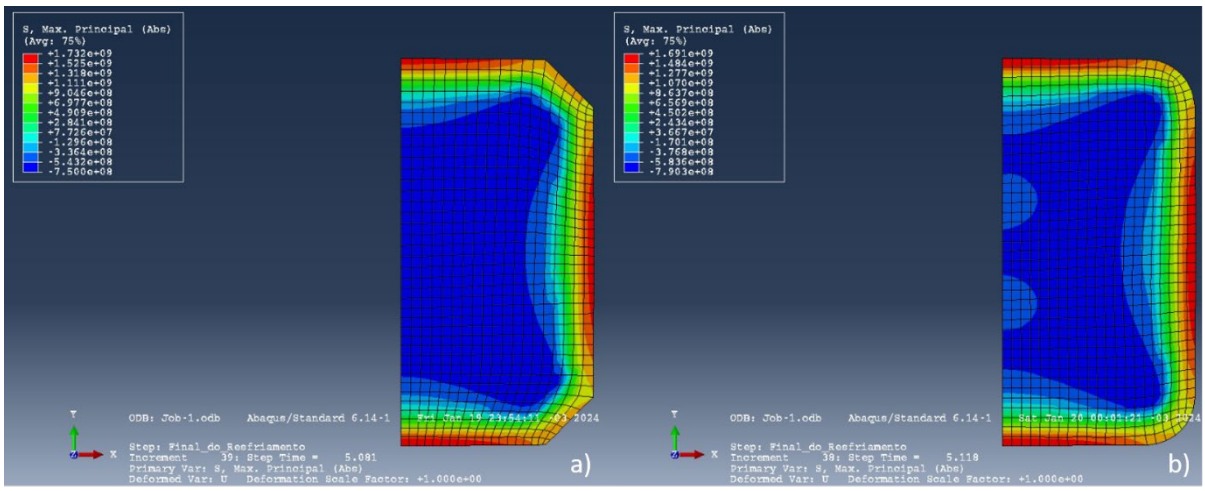

Figure 26 – Simulation step where the stresses reached their maximum values in the axisymmetric model of the cylinder's half cross-section with a) chamfering and b) rounding.

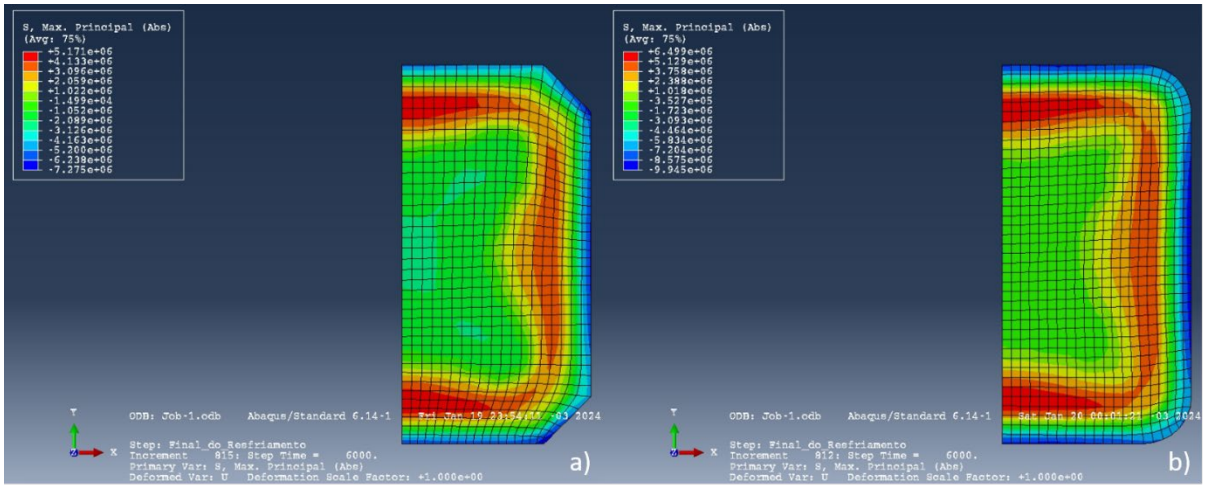

Figure 27 – Simulation step where the stresses reached their final values in the axisymmetric model of the cylinder's half cross-section with a) chamfering and b) rounding.

Figures 26 and 27 show that the maximum tensile and compressive stresses are formed in other regions (face, bulk) and not in the corners. This can be explained because the stress generated in a surface element depends on its distance to the interior that is compressing. As the vertex of a square is the furthest point from its midpoint, the edges and vertices of the models are less influenced by these stresses, as shown in Figure 28.

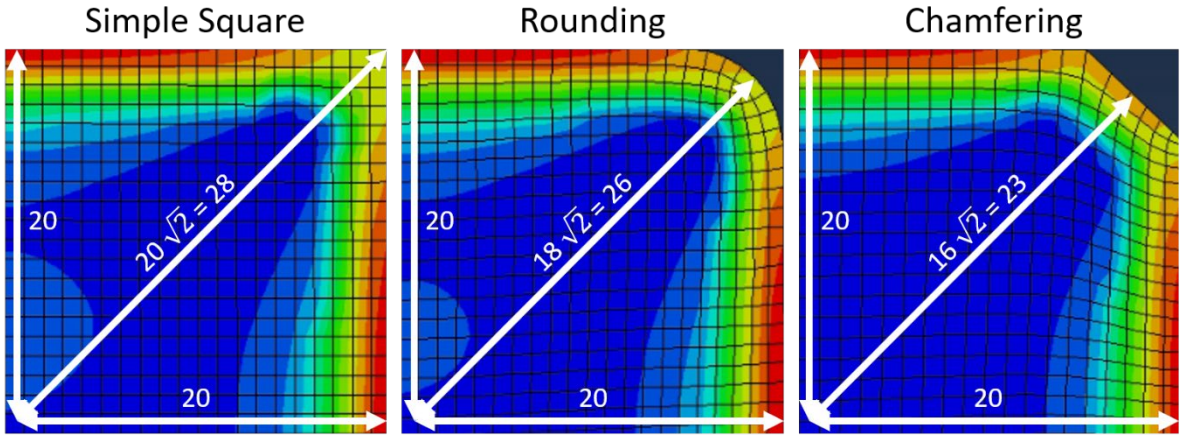

Figure 28 – Illustration of the distance from the center of the sample to its face and vertex.

Table 7 – Values obtained by the axisymmetric cylinder chamfering/rounding analysis, represented in red or green when, respectively, above or below the mechanical strength of the soda-lime glass.

Cooling Rate: 77.5 °C	Axisym. Cylinder [MPa]	Axisym. with Chamfering [MPa]	Axisym. with Rounding [MPa]	Mechanical Strength [MPa]
Maximum Tensile Stress	1671	1732	1691	33
Max. Compression Stress	1372	1359	1366	326
Final Tensile Stress	6	5	6	33
Final Compression Stress	8	7	10	326

In Table 7, it is clear that chamfering and rounding actually increased the maximum tensile and compressive stresses. One possible explanation is that these methods reduce the surface area of the faces, concentrating the stresses generated in these other regions.

4.3.2 Effect of Chamfering/Rounding on Smartphone Screen Protector - 3D

Figures 29 and 30 show, respectively, the instants during simulation when the stresses reached their maximum and final values (at the end of the simulation) in the 3D model of the 1/4 smartphone screen protector with chamfering/rounding. The values are compared in Table 8.

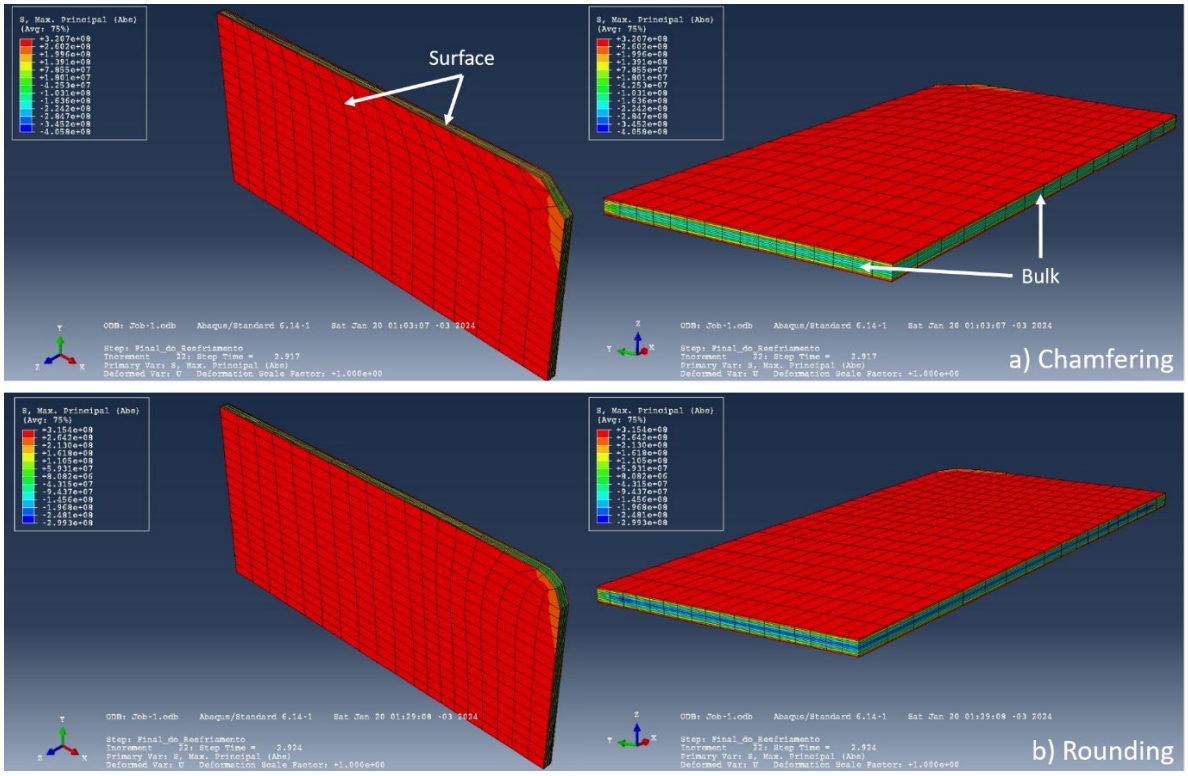

Figure 29 – Simulation step where the stresses reached their maximum values in the 3D model of the 1/4 smartphone screen protector with a) chamfering and b) rounding.

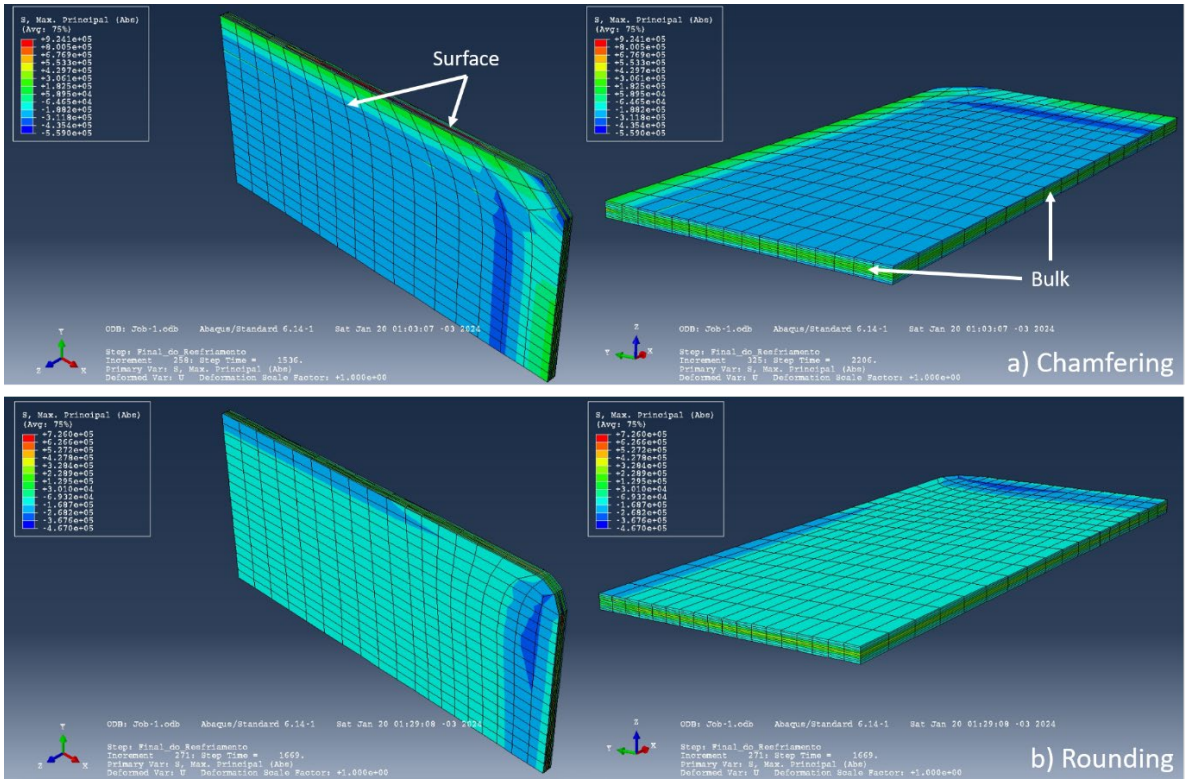

Figure 30 – Simulation step where the stresses reached their final values in the 3D model of the 1/4 smartphone screen protector with a) chamfering and b) rounding.

Table 8 – Values obtained by the 3D screen protector chamfering/rounding analysis, represented in red or green when, respectively, above or below the mechanical strength of the soda-lime glass.

Cooling Rate: 77.5 °C	3D Screen [MPa]	3D with Chamfering [MPa]	3D with Rounding [MPa]	Mechanical Strength [MPa]
Maximum Tensile Stress	323	321	315	33
Maximum Compression Stress	300	407	299	326
Final Tensile Stress	0.7	0.9	0.7	33
Final Compression Stress	0.6	0.6	0.5	326

Table 8 shows that only chamfering increased the maximum tensile and compressive stresses in the 3D model, while rounding had values very close to the original model.

4.4 EFFECT OF COOLING RATE

The results of 3.2 FEM MODELS cooling rate analysis are presented below. The critical cooling rates were defined and the results were compared with those obtained in the initial condition (cooling rate of 77.5 °C/s).

4.4.1 Effect of Cooling Rate on Cylinder's Half Cross-Section - Axisymmetric

Figures 31 and 32 show, respectively, the instants during simulation when the stresses reached their maximum and final values (at the end of the simulation) in the axisymmetric model of the cylinder's half cross-section. The maximum tensile stress equaled the tensile strength of the soda-lime glass when cooling from 800 °C to 25 °C was achieved in 4125 seconds, *i.e.*, at a critical cooling rate of ~0.2 °C/s. The values are compared in Table 9.

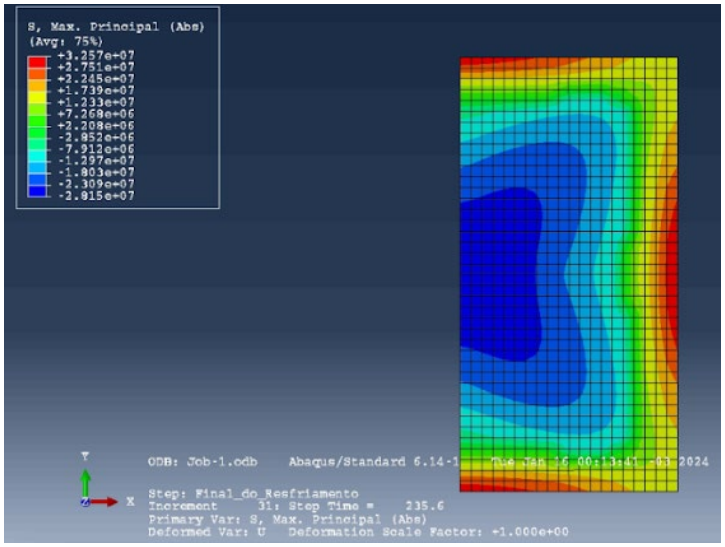

Figure 31 – Simulation step where the stresses reached their maximum values in the axisymmetric model of the cylinder's half cross-section.

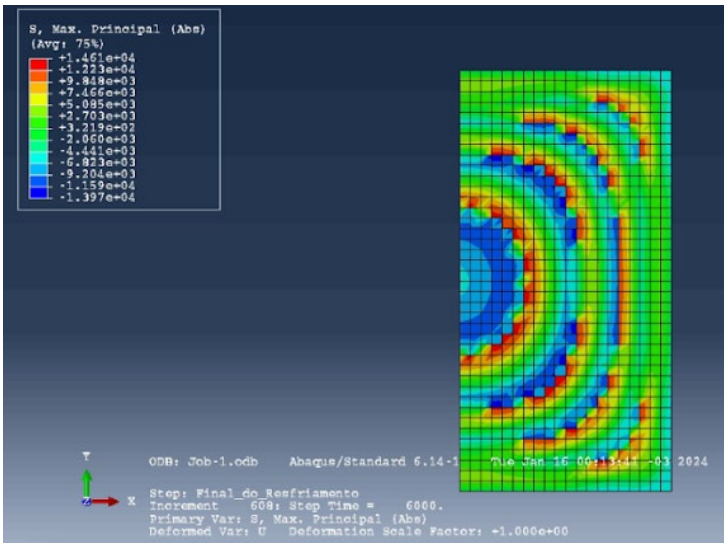

Figure 32 – Simulation last step where the stresses reached their final values in the axisymmetric model of the cylinder's half cross-section.

Table 9 – Values obtained by the axisymmetric cylinder cooling rate analysis, represented in red or green when, respectively, above or below the mechanical strength of the soda-lime glass.

	Axisymmetric Cylinder at 77.5 °C/s [MPa]	Axisymmetric Cylinder at 0.2 °C/s [MPa]	Mechanical Strength [MPa]
Maximum Tensile Stress	1671	33	33
Maximum Compression Stress	1372	28	326
Final Tensile Stress	6	0.02	33
Final Compression Stress	8	0.01	326

As Table 9 shows, all the stresses generated during tempering at a cooling rate of 0.2 °C/s are contained in the material's mechanical strength range.

Figure 32 shows the formation of stress striations, which usually occur experimentally when large-volume glass samples are solidified. This may be a further indication that the simulation is qualitatively correct. However, as mentioned earlier, the model does not yet have quantitative accuracy and therefore it cannot be assumed that there would be this number of striations, with this same size and intensity.

4.4.2 Effect of Cooling Rate on Smartphone Screen Protector - 3D

Figures 33 and 34 show, respectively, the instants during simulation when the stresses reached their maximum and final values (at the end of the simulation) in the 3D model of the 1/4 smartphone screen protector. The maximum tensile stress equaled the tensile strength of the soda-lime glass when cooling from 800 °C to 25 °C was achieved in 106 seconds, *i.e.*, at a critical cooling rate of ~7 °C/s. The values are compared in Table 10.

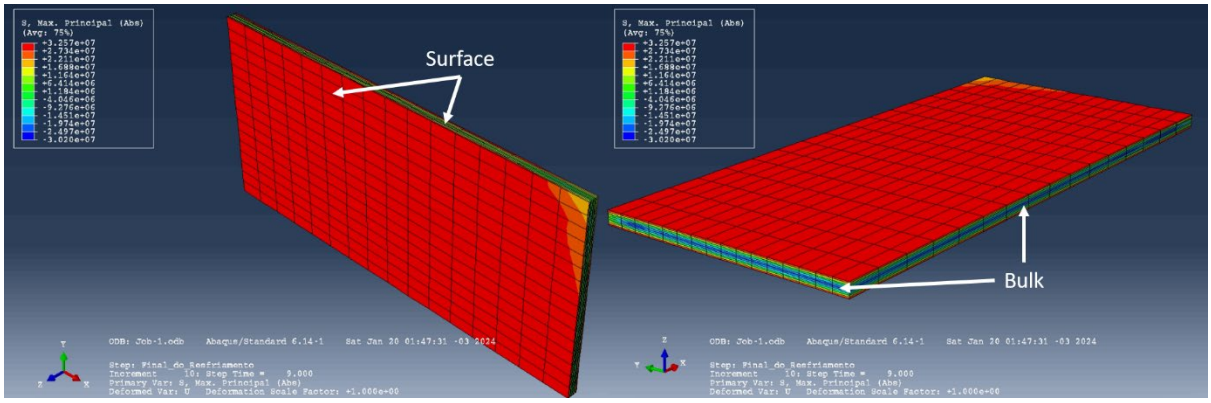

Figure 33 – Simulation step where the stresses reached their maximum values in the 3D model of the 1/4 smartphone screen protector.

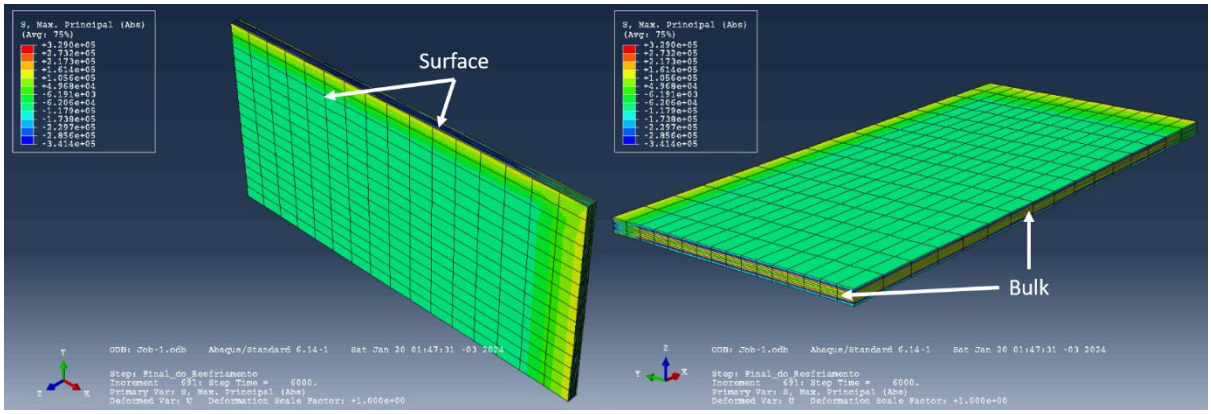

Figure 34 – Simulation last step where the stresses reached their final values in the 3D model of the 1/4 smartphone screen protector.

Table 10 – Values obtained by the 3D screen protector cooling rate analysis, represented in red or green when, respectively, above or below the mechanical strength of the soda-lime glass.

	3D Screen at 77.5 °C/s [MPa]	3D Screen at 7 °C/s [MPa]	Mechanical Strength [MPa]
Maximum Tensile Stress	323	33	33
Maximum Compression Stress	300	30	326
Final Tensile Stress	0.7	0.3	33
Final Compression Stress	0.6	0.3	326

As Table 10 shows, all the stresses generated during tempering at a cooling rate of 7 °C/s are contained in the material's mechanical strength range. However, as mentioned earlier, the values of critical cooling rate do not yet have quantitative accuracy because of the simplifications of the model.

The large difference in critical cooling rate between the axisymmetric cylinder and the 3D screen shows that bulky samples are more sensitive to the critical cooling rate. Samples with geometries similar to screens or plates will have a smaller temperature gradient between the surface and their bulk, making it possible to cool them at much higher rates.

5 DISCUSSION

The simulation of glass tempering via Finite Element Analysis was performed using the subroutine UEXPAN to predict the thermal expansion coefficients for each element during cooling. However, although the simulation represented various phenomena that had been observed experimentally, it can exclusively be used for qualitative analysis. To be able to quantitatively calculate these values and compare them with real data, the model must be enhanced to predict the phenomena of stress relaxation in the liquid phase combined with the variation in Tg as a function of the cooling rate in each node, as well as contain mechanical and thermal properties' variation with the temperatures present in the process.

The mesh convergence analysis indicated that the number of mesh elements needed to converge the data is directly proportional to the complexity of the mesh. The 2D model meshes converged at similar values of mesh elements (~1000), while the 3D mesh needed about twice as many (~2500).

The stress history of the models was compared with the strength of the soda-lime glass mechanical strength envelope, making it possible to predict whether the sample would fracture at a given cooling rate. It was observed that the maximum tensile and compressive stresses occur during the cooling dynamics of tempering, and that the final stresses represent 1% to 10% of the value of the maximum stresses. This shows the importance of analyzing the entire stress history to predict material fracture, and not just the equilibrium stresses at the end of glass tempering simulation.

The geometry analysis showed that samples with a large internal volume led to a higher temperature gradient between the bulk and the surface, which results in higher stresses. In the 2D analysis, the stress values in the cylinder model exceeded those of the smartphone screen protector by 1 order of magnitude. In the 3D analysis, the cylinder model needed a much lower cooling rate than the smartphone screen protector to obtain the same maximum tensile stress. In general, the higher the surface/volume ratio, the easier it is to perform tempering without fracturing the material. Samples with geometries similar to screens or plates will have a smaller temperature gradient between the surface and their bulk, making it possible to cool them at much higher rates. As expected by the thermal shock theory.

The geometry used in the model alters the analysis values, as does the type of model (axisymmetric or three-dimensional). The stresses simulated in the 3D model of smartphone screen protector were greater than those obtained in the axisymmetric model. This effect may be a consequence of the boundary conditions not being exactly the same for each model dimension (for example, the axisymmetric model may have a larger surface area, just as the 3D model may contain different values near the outer edges on the Z axis, etc.).

The simulated stress evolution is in accordance with the theoretical prediction. Initially, the thermal contraction of the surface is greater than that of the bulk, producing tensile stresses on the surface and compressive stresses internally. The bulk then cools more quickly than the surface and the thermal contraction of the bulk exceeds that of the surface, producing tensile stresses in the bulk and compressive stresses on the surface. It was also possible to visualize the moment when the stresses cancel each other out. However, as the model does not predict stress relaxation, it is likely that the model accumulated all the internal stresses generated in the liquid interior.

As expected, the cooling rate has a direct impact on the stresses generated during tempering. The model also proved capable in predicting the critical cooling rates for each sample, ensuring that the material does not fracture. It was observed that the factor with the greatest impact is the surface/volume ratio. While the cylinder with dimensions of 20 x 20 x 20 mm needed 4125 seconds to solidify without fracturing, the smartphone screen protector with dimensions of 164 x 76 x 2 mm needed only 106 seconds, *i.e.*, a rate of ~7 °C/s. This cooling rate is within the range of values obtainable via air cooling, usually between 1 and 10 °C/s. However, as mentioned earlier, the values of the critical cooling rate still lack quantitative precision due to the simplifications of the model.

Another indication that the simulation is qualitatively correct was the formation of tension striations when the cylinder was cooled to ~0.2 °C/s, a phenomenon that occurs experimentally when large-volume glass samples are solidified. However, the number of striations, their sizes and intensities can only be predicted in a more refined model.

Despite the above, some results contrasted with what had been expected. In general, chamfering and rounding actually increased the maximum tensile and compressive stresses generated in all the analyses. The hypothesis established in this work is that these methods reduce the surface area of the faces, concentrating the stresses generated in these other regions.

In addition, the tensile and compressive stresses were accumulated in other regions (face, bulk) and not in the corners of the samples. The hypothesis established in this work is that the stress generated in a surface element depends on its distance from the bulk that is compressing. As the vertices and edges of the samples are always further away from the interior than the faces, there is less response to contraction stresses from the bulk, generating lower stresses in the corners of the samples.

6 CONCLUSIONS/FINAL CONSIDERATIONS

In this work, it was demonstrated that it is possible to simulate glass tempering via the Finite Element Method.

The analysis of the entire stress history produced during tempering was shown to be useful to prevent material fracture, since the maximum tensile and compressive stresses appear long before the entire sample reaches room temperature. The residual stresses in the samples at the end of tempering represent only about 1-10% of these maximum stresses.

The analysis showed that the stresses generated depend on various factors such as sample geometry, analysis type (axisymmetric or 3D), cooling rate and surface/volume ratio.

Depending on the analysis type, the boundary conditions are not exactly the same. Slower cooling reduces the intensity of the stresses generated. The higher the surface/volume ratio, the higher the critical cooling rate and the easier it is to perform tempering without fracturing the sample. It was estimated rates of up to ~7 °C/s to produce smartphone screen protectors, making it possible to temper them in air.

It was hypothesized that the edges/vertices suffer less impact from the bulk contraction because they are always further away from it than the faces, where the maximum stresses occur. Thus, chamfering and rounding corners reduces the area of these faces and concentrates stresses in other regions (face, bulk).

An interesting aspect of the work was the possibility of visually studying, step by step, the stress evolution. Initially, there was greater thermal contraction on the outside of the sample, followed by greater thermal contraction on the inside, resulting in the well-known profile of compressive stresses on the surface and tensile stresses in the bulk.

Finally, the finite element simulation showed good qualitative accuracy, exhibiting some phenomena predicted by the theory, such as the inversion of stresses during tempering, or that actually occur in practice, such as stress striations in bulky samples.

For future work, it is suggested the enhancement of this model with the stress relaxation in the liquid phase and in the solid phase during glass transition, as well as the variation of Tg as a function of cooling rate. If this is implemented in the model, it will be possible to obtain quantitative results.

REFERENCES

BARTENEV, G. M. Tempering of Glass. **Zh. Tekhn. Fiz.**, v. 19, n. 12, p. 33-1423, 1949.

BATHE, K.J. **Finite Element Method**. John Wiley & Sons, 2008.

CHOI, Y. S.; YUN, J. U.; PARK, S. E. Flat panel display glass: Current status and future. **Journal of Non-Crystalline Solids**, v. 431, p. 2-7, 2016.

DAVIS, M. J.; ZANOTTO, E. D. Glass-ceramics and realization of the unobtainable: Property combinations that push the range. **MRS Bulletin**, v. 42, n. 3, p. 195-199, 2017.

GARDON, R. Thermal Tempering of Glass. **Glass Science and Technology**, v. 5, n. 5, p. 145-216, 1980.

GOTTSMANN, J.; DINGWELL, D. B.; GENNARO, C. Thermal expansion of silicate liquids: direct determination using container-based dilatometry. **American Mineralogist**, v. 84, n. 7-8, p. 1176-1180, 1999.

GUGLIELMO, C. **Corning, After Thinning Out Gorilla Glass, Makes New Generation Tougher**, 2013. Available on: <https://www.forbes.com/sites/connieguglielmo/2013/01/10/corning-after-thinning-out-gorilla-glass-makes-new-generation-tougher/#4b3a28426759>. Accessed Janv 14, 2024.

HÖLAND, W.; BEALL, G. H. **Glass-ceramic technology**. John Wiley & Sons, 2019.

LEE, E. H.; ROGERS, T. G.; WOO, T. C. Residual Stresses in a Glass Plate Cooled Symmetrically from Both Surfaces. **Journal of the American Ceramic Society**, v. 48, n. 9, p. 480-487, 1965.

LIU, S. F.; CHANG, C. F.; WANG, M. H.; LAI, H. H. A Study of the Factors Affecting the Usability of Smart Phone Screen Protectors for the Elderly. **Lecture Notes in Computer Science**, v. 9754, p. 457-465, 2016.

NARAYANASWAMY, O. S.; GARDON, R. Calculation of Residual Stresses in Glass. **Journal of the American Ceramic Society**, v. 52, n. 10, p. 554-558, 1969.

TELECO. **Vendas no mundo**, 2014. Available on: <http://www.teleco.com.br/pais/celprodw.asp>. Accessed Janv 14, 2024.

VARSHNEYA, A. K. **Fundamentals of inorganic glasses**. Elsevier, 2013.

VOGEL, W. **Structure and crystallization of glasses**. Pergamon Press, 2013.

ZANOTTO, E. D.; MAURO, J. C. The glassy state of matter: Its definition and ultimate fate. **Journal of Non-Crystalline Solids**, v. 471, p. 490-495, 2017.

APPENDIX A – ABAQUS UEXPAN Subroutine for calculating CTE within the glass transition range

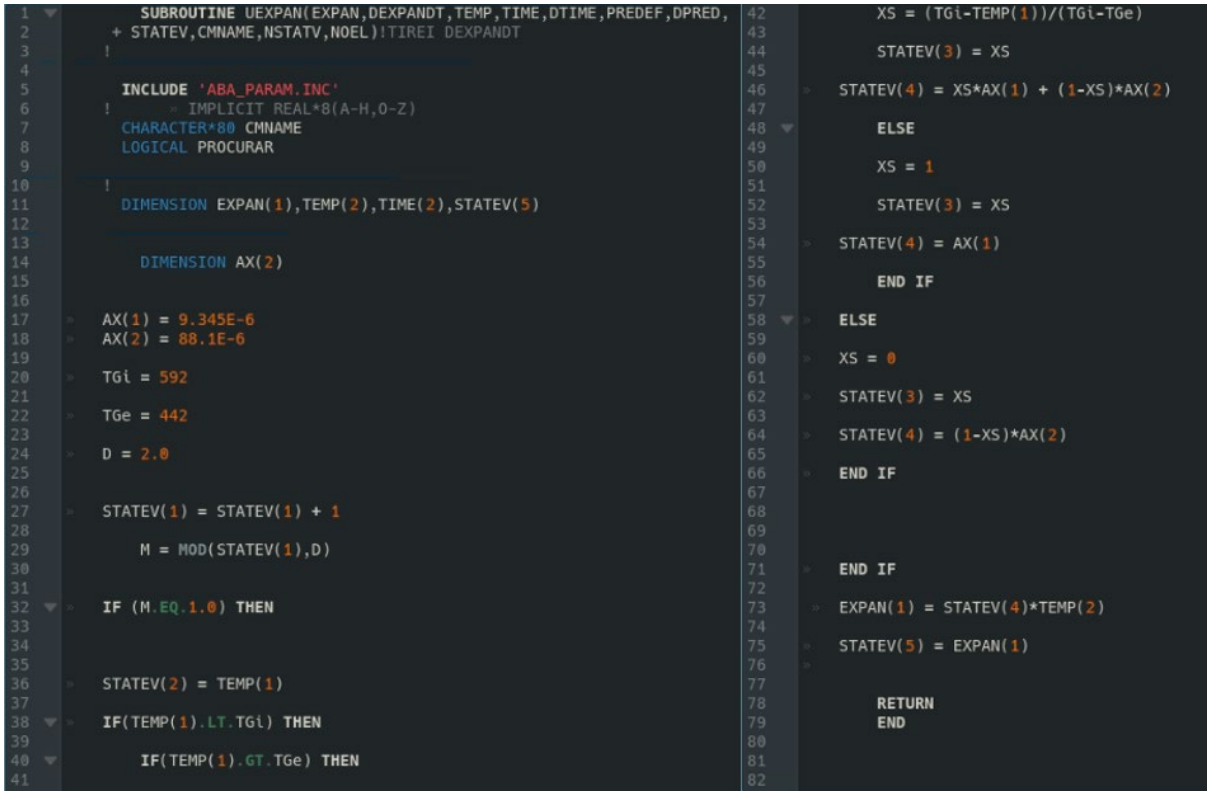

```
      SUBROUTINE UEXPAN(EXPAN,DEXPANDT,TEMP,TIME,DTIME,PREDEF,DPRED,
     + STATEV,CMNAME,NSTATV,NOEL)!TIREI DEXPANDT
     !

      INCLUDE 'ABA_PARAM.INC'
     !      IMPLICIT REAL*8(A-H,O-Z)
      CHARACTER*80 CMNAME
      LOGICAL PROCURAR

     !
      DIMENSION EXPAN(1),TEMP(2),TIME(2),STATEV(5)


        DIMENSION AX(2)


    AX(1) = 9.345E-6
    AX(2) = 88.1E-6

    TGi = 592

    TGe = 442

    D = 2.0


    STATEV(1) = STATEV(1) + 1

        M = MOD(STATEV(1),D)


    IF (M.EQ.1.0) THEN



    STATEV(2) = TEMP(1)

    IF(TEMP(1).LT.TGi) THEN

        IF(TEMP(1).GT.TGe) THEN

            XS = (TGi-TEMP(1))/(TGi-TGe)

            STATEV(3) = XS

    STATEV(4) = XS*AX(1) + (1-XS)*AX(2)

        ELSE

            XS = 1

            STATEV(3) = XS

    STATEV(4) = AX(1)

        END IF

    ELSE

    XS = 0

    STATEV(3) = XS

    STATEV(4) = (1-XS)*AX(2)

    END IF



    END IF

    EXPAN(1) = STATEV(4)*TEMP(2)

    STATEV(5) = EXPAN(1)


        RETURN
        END
```

To copy and paste, containing all spaces and tabs:

```
      SUBROUTINE UEXPAN(EXPAN,DEXPANDT,TEMP,TIME,DTIME,PREDEF,DPRED,
     + STATEV,CMNAME,NSTATV,NOEL)!TIREI DEXPANDT
     !

      INCLUDE 'ABA_PARAM.INC'
     !      IMPLICIT REAL*8(A-H,O-Z)
      CHARACTER*80 CMNAME
      LOGICAL PROCURAR

     !
      DIMENSION EXPAN(1),TEMP(2),TIME(2),STATEV(5)


        DIMENSION AX(2)


          AX(1) = 9.345E-6
          AX(2) = 88.1E-6

          TGi = 592

          TGe = 442

          D = 2.0
```

```
    STATEV(1) = STATEV(1) + 1
M = MOD(STATEV(1),D)

    IF (M.EQ.1.0) THEN


    STATEV(2) = TEMP(1)
    IF(TEMP(1).LT.TGi) THEN
IF(TEMP(1).GT.TGe) THEN
XS = (TGi-TEMP(1))/(TGi-TGe)
STATEV(3) = XS
    STATEV(4) = XS*AX(1) + (1-XS)*AX(2)
ELSE
XS = 1
STATEV(3) = XS
    STATEV(4) = AX(1)
END IF
    ELSE
    XS = 0
    STATEV(3) = XS
    STATEV(4) = (1-XS)*AX(2)
    END IF


    END IF
    EXPAN(1) = STATEV(4)*TEMP(2)
    STATEV(5) = EXPAN(1)

RETURN
END
```